Mon. Not. R. astr. Soc. (1978) **183**, 367–395

The destruction and growth of dust grains in interstellar space – I. Destruction by sputtering

Michael J. Barlow★ *Astronomy Centre, University of Sussex, Brighton BN1 9QH*

Received 1977 October 3; in original form 1977 July 15

Summary. The processes governing the destruction and growth of dust grains in interstellar space are investigated with a view to establishing the conditions required for the existence of ice mantles. In this paper sputtering by particles with energies in the eV to GeV range is considered. Previous sputtering yield estimates which were based on theoretical considerations are shown to be greatly in error for incident particle energies of less than 1 keV. Empirical formulae for the sputtering threshold energy and the sputtering yield are derived from the extensive experimental data available. The sputtering of grains in H II regions, in the inter-cloud medium, and in shock waves produced by cloud–cloud collisions and by supernova remnants, is investigated. Of these, supernova remnants are shown to be the most important, leading to lifetimes of $\sim 2 \times 10^8$ yr for ice grains and between $5–20 \times 10^8$ yr for refractory grains. Destruction rates are estimated for grains bombarded by MeV and GeV cosmic rays. It is shown that collision cascade sputtering dominates evaporative sputtering produced by thermal spikes. It is also shown that even if all the electron excitation energy loss in a grain material could be transferred to the lattice particles, the observed cosmic ray flux spectrum could not cause significant destruction of ice grains.

1 Introduction

The problem of the processes governing the growth and destruction of interstellar dust grains was first discussed in detail by Oort & van de Hulst (1946), on the basis of the dirty-ice accretion model of van de Hulst (1943). They concluded that the growth of an ice grain to a radius of 10^{-5} cm in 10^8 yr would be balanced by its destruction once every 10^8 yr by a collision with another grain during the head-on collision of two interstellar clouds. This model appeared to satisfy existing constraints on the properties of interstellar dust, since unrestricted growth of dust grains was not consistent with observations.

The dirty-ice model of interstellar grains was modified with the suggestion by Hoyle &

★ Present address: Joint Institute for Laboratory Astrophysics, University of Colorado and National Bureau of Standards, Boulder, Colorado 80309, USA.

Wickramasinghe (1962) that carbon stars could inject graphite grains into the interstellar medium; Kamijo (1963) similarly suggesting that oxygen-rich late-type stars could provide a source of silicate grains. Wickramasinghe (1965) investigated the growth and destruction processes governing the accretion of ice mantles on such refractory grains, suggesting that sputtering, as well as grain–grain collisions, could be an important destruction process. A severe blow to interstellar ice-grain models was dealt by the failure of Danielson, Woolf & Gaustad (1965) and Knacke, Cudaback & Gaustad (1969) to detect the predicted 3.1 μm absorption band of water ice towards several highly reddened stars. This band has since been detected, starting with Gillett & Forrest (1973), but always only in the direction of dense molecular clouds. Gillett *et al.* (1975) obtained an exceedingly low upper limit to the strength of the 3.1 μm feature towards the highly reddened star VI Cyg no. 12, which is thought to be reddened by dust which is typical of the diffuse interstellar medium. The problem therefore exists of explaining the lack of ice mantles in the diffuse interstellar medium and their confinement to dense molecular clouds.

In this and the following paper the possible processes governing the destruction of ice mantles in the interstellar medium are considered in turn (in addition to the destruction processes affecting refractory grains). In general, three possible values of the sublimation energy H_s of ice grains (H_s is the mean energy required to remove one lattice molecule from a grain surface) will be considered when discussing destruction mechanisms. These are: $H_s = 0.1$ eV (implied by the work of Hunter & Donn (1971) on the co-adsorption of NH_3, H_2O and CH_4 mixtures, *cf.* Section III of Paper 2); $H_s = 0.18$ eV (the classical value of Oort & van de Hulst (1946), derived from thermodynamic data); and $H_s = 0.37$ eV (the value derived by de Jong & Kamijo (1972, unpublished) using more recent thermodynamic data). Emphasis will generally be placed on the results for $H_s = 0.1$ eV, since these provide upper limits to destruction rates.

2 Types of sputtering

Sputtering may be defined as a process whereby lattice particles in a solid material are ejected by bombarding atoms or ions. This ejection normally occurs by means of a billiard ball-type sequence of collisions between an incoming ion and lattice particles, resulting in a certain probability of a lattice particle receiving sufficient energy to overcome the binding potential of the solid. The minimum bombarding particle energy needed for sputtering to occur is normally called the threshold energy, E_T. Following Pease (1960); Wickramasinghe (1972) has discussed the three energy regimes for sputtering: (1) The hard-sphere collision regime, operative when the bombarding particle has energy E less than E_A (E_A is defined in Section 4.2 and is normally ~ a few keV). (2) The screened Coulomb collision regime, operative when $E_A < E < E_B$ (E_B is also defined in Section 4.2, and typical values of E_A and E_B for interstellar grain materials are given in Table 7). In the screened Coulomb regime the interaction is partially Coulombic, although some of the nuclear charge is still screened by the electron shell. (3) The Rutherford collision regime, operative when $E > E_B$ (e.g. in the MeV region). In this case collisions are purely Coulombic. The behaviour of the sputtering yield Y (Y = number of lattice particles ejected per incident particle) in these energy regimes is such that Y increases linearly from zero at $E = E_T$ to a maximum at $E = E_A$. Between $E = E_A$ and $E = E_B$ the yield is relatively constant, falling slightly with increasing E, and for $E > E_B$ the yields falls as $\ln(E)/E$.

Numerous authors has investigated whether low energy sputtering (i.e. E ~ few eV, as in shock waves or H II regions) could be of importance in the destruction of ice grains, and some have concluded that it would be important. We reconsider the entire question of low

energy sputtering in Section 3, in particular showing that no existing theories are adequate for predicting sputtering yields for $E < E_A$, and that empirical yields derived from experiment must be used instead. In Section 4 sputtering yields are derived for bombarding particles with $E > E_A$ (i.e. keV and MeV particles), using the sputtering theory of Pease (1960). Other sputtering mechanisms more esoteric than collision cascade sputtering may be operative in certain situations, one of these being the thermal spike mechanism, whereby energy deposited on a short timescale in a small volume can lead to a large local temperature rise, with possible resultant evaporation of lattice particles if the heated volume intersects the surface. The possible importance of such thermal spikes in the destruction of ice grains is also considered in 4. In both Sections 3 and 4 the sputtering yields derived for the appropriate energy regimes are used to estimate the importance of sputtering in varied astrophysical situations.

The above type of sputtering may be termed physical sputtering. Destruction of a solid surface by chemical reactions between bombarding particles and the lattice material might possibly occur also. Various types of grain surface reaction destruction mechanisms are considered separately in Paper II.

3 Low-energy sputtering

3.1 INTRODUCTION

Wickramasinghe (1965) made the first attempt to estimate the effects of low-energy sputtering on interstellar grains, basing his work on Wehner's (1957) empirical relationship which treated sputtering as a momentum transfer process. However, as noted by Mathews (1969), it was shown experimentally by Wehner (1958) that the sputtering yield of a material was proportional to the *energy* of the incident ion. Wehner (1958) derived the following empirical relationship for the sputtering yield Y:

$$Y = K(E - E_T) \tag{1}$$

where E is the energy of the incident ion, E_T is a threshold energy below which no sputtering occurs and K is a constant, for a particular ion–solid combination, called the sputtering yield slope. Mathews (1969) used a relationship for the sputtering yield based on this formula, with an estimate for the threshold energy based on the theoretical work of Langberg (1958). Unfortunately the value of the sputtering yield slope was seriously overestimated in Mathews (1969), as pointed out by Barlow (1971). Aannestad (1973) produced a treatment for low-energy sputtering based on collision dynamics considerations. Burke & Silk (1974) considered the sputtering of graphite grains in a hot gas.

We will show here that all existing theories of low-energy sputtering lead to predictions which are in serious disagreement with the experimental data, and that the only safe way of estimating low-energy sputtering yields for interstellar grain materials is by empirical deduction from the existing experimental data. In Section 3.2 we derive an empirical relationship for the sputtering threshold energy and in 3.3 we do likewise for the sputtering yield slope. These results are then applied in successive sections to estimate, for a variety of grain materials, sputtering rates in a hot gas, in H II regions, in the inter-cloud medium and in shock waves.

3.2 THE SPUTTERING THRESHOLD ENERGY

Using highly sensitive techniques Stuart & Wehner (1962) measured sputtering threshold energies for 117 different ion–target combinations, using ions of Ne, Ar, Xe, Kr and Hg at

normal incidence. They noted that the threshold energies were approximately equal to $4H_s$, where H_s is the sublimation energy of a lattice particle of the solid. This value also corresponds to the value of the threshold displacement energy, E_d, for lattice particles in a solid (Seitz 1949). The low-energy sputtering theories of Henschke (1957) and Langberg (1958) both predicted that the threshold energy at *normal* incidence would be of the form

$$E_T(\perp) = \frac{4H_s}{\eta_i} \cdot \kappa \qquad (2)$$

where the energy transfer factor η_i is given by $\eta_i = 4m_iM_s/(m_i + M_s)^2$, with m_i the mass of the impinging ion and M_s the mass of a lattice particle. η_i thus can have a maximum value of unity. The constant κ was predicted to be between 2.5 and 3.5 by Henschke (1957) and to be between 2 and 5 by Langberg (1958). We note that the measured threshold energies at normal incidence (see Table 1) are thus considerably less than those predicted.

The theory of Langberg (1958) was only applicable for the special case of normally incident ions, but the theories of Henschke (1957) and Harrison & Magnusson (1961) predicted, and the expressions used by Mathews (1969), Barlow (1971) and Aannestad (1973), assumed, that the threshold energy has a strong dependence on the angle of incidence of the incoming ion, using the dynamical argument that it ought to be easier to knock off a surface atom at grazing incidence than at normal incidence. However, the ultrasensitive work of

Table 1. Threshold energy data★.

		Ne$^+$				Ar$^+$			
Target	H_s (eV)	E_T (eV)	η_i	$E_T\eta_i/H_s$	E_T/H_s	E_T (eV)	η_i	$E_T\eta_i/H_s$	E_T/H_s
Be	3.38	12	0.86	3.1	3.6	15	0.6	2.6	4.4
Al	3.37	13	0.98	3.8	3.9	13	0.96	3.7	3.9
Ti	4.87	22	0.83	3.7	4.5	20	0.99	4.1	4.1
V	5.32	21	0.81	3.2	3.9	23	0.99	4.3	4.3
Cr	4.11	22	0.80	4.3	5.4	22	0.98	5.3	5.4
Fe	4.3	22	0.78	4.0	5.1	20	0.97	4.6	4.7
Co	4.39	20	0.76	3.5	4.6	25	0.96	5.5	5.7
Ni	4.44	23	0.76	3.9	5.2	21	0.96	4.5	4.7
Cu	3.5	17	0.73	3.5	4.9	17	0.95	4.7	4.9
Ge	3.89	23	0.68	4.0	5.9	25	0.92	5.9	6.4
Zr	6.29	23	0.59	2.2	3.7	22	0.85	3.0	3.5
Nb	7.49	27	0.58	2.1	3.6	25	0.84	2.8	3.3
Mo	6.82	24	0.57	2.0	3.5	24	0.83	2.9	3.5
Rh	5.75	25	0.55	2.4	4.3	24	0.81	3.4	4.2
Pd	3.93	20	0.53	2.7	5.1	20	0.80	4.1	5.1
Ag	2.95	12	0.53	2.2	4.1	15	0.79	4.0	5.1
Ta	8.09	25	0.36	1.1	3.1	26	0.59	1.9	3.2
W	8.74	35	0.35	1.4	4.0	33	0.59	2.2	3.8
Re	7.99	35	0.35	1.5	4.4	35	0.58	2.6	4.4
Pt	5.85	27	0.34	1.6	4.6	25	0.57	2.5	4.3
Au	3.82	20	0.33	1.7	5.2	20	0.56	3.0	5.2
Th	5.91	20	0.29	1.0	3.4	24	0.50	2.0	4.1
U	5.47	20	0.29	1.1	3.7	23	0.49	2.1	4.2
Mean				3.0	4.3			3.55	4.45
Standard deviation (σ)				2.05	0.75			1.2	0.8
r = mean/σ				1.46	5.73			2.96	5.6

★ Sputtering threshold energies, E_T, taken from Stuart & Wehner (1962).

Cuderman & Brady (1968), with Ar^+ ions incident on Ni, shows definitively that the threshold energy has virtually no dependence on the angle of incidence, varying between $E_T = 18\,eV$ ($4.05\,H_s$) and $E_T = 25\,eV$ ($5.6\,H_s$) over a range in the angle of incidence of 60°. This variation of the threshold energy (the two values in fact overlap within the statistical errors) is considerably less than the large variation with angle predicted in the various papers named above.

Since, contrary to theoretical expectations, there is no angular dependence of the threshold energy, we might ask if the dependence of E_T on the energy transfer factor η_i, which is predicted in (2), is in fact present in the experimental results. Table 1 lists the threshold energy data for Ne^+ and Ar^+ ions incident normally on various target materials. Column 1 lists the target material and column 2 lists the sublimation energy H_s. The next four columns then list, for the case of incident Ne^+ ions, the measured threshold energy E_T from Stuart & Wehner (1962), the energy transfer factor η_i, the quantity $E_T\eta_i/H_s$, and the quantity E_T/H_s. The same four quantities are then listed in the next four columns for the case of incident Ar^+ ions. It is immediately obvious from Table 1 that when η_i is less than 0.7 the quantity $E_T\eta_i/H_s$ declines rapidly with decreasing η_i, rather than remaining constant as predicted by (2); whereas the quantity E_T/H_s remains relatively constant with changing η_i. Quantitatively, for incident Ne^+ ions the ratio r of the mean to the standard deviation is equal to 1.5 for the quantity $E_T\eta_i/H_s$, whereas r is equal to 5.7 for the quantity E_T/H_s. For incident Ar^+ ions r is equal to 3.0 for $E_T\eta_i/H_s$, and equal to 5.6 for E_T/H_s, the smaller difference being attributable to the smaller number of ion–target combinations with $\eta_i < 0.7$. The data for incident Kr^+, Xe^+ and Hg^+ ions (not listed because of the small number of combinations with $\eta_i < 0.7$) are also in agreement with the trends for Ne^+ and Ar^+ ions. We note that Furr & Finfgeld (1970) have measured a significant sputtering yield for 500 eV protons incident on Au, whereas the relation $E_T = 4H_s/\eta_i$ would predict a threshold energy of 764 eV for this ion–target combination ($\eta_i = 0.02$), with no sputtering at 500 eV. If on the other hand the threshold energy is equal to $4H_s$, as found from the experimental results of Stuart & Wehner (1962), then the results of Furr & Finfgeld (1970) can be understood.

All of the experimental results on threshold energies so far discussed have been for monatomic solids. However, Jorgenson & Wehner (1965) have measured a threshold energy of 16 eV for Ar^+ ions incident on quartz (SiO_2), corresponding to $E_T = 3.6H_s$. We conclude that the following expression should reasonably represent the threshold energy for all materials.

$$E_T = 4\,H_s. \tag{3}$$

Since the threshold energy shows no dependence upon the angle of ion incidence or upon the energy transfer factor η_i, it would appear that the sputtering ejection mechanism at low energies must be by means of some process of resonance energy transfer rather than by means of binary billard ball collision sequences envisaged in existing theories of low-energy sputtering.

3.3 THE SPUTTERING YIELD SLOPE

We now determine values of the sputtering yield slope appropriate for interstellar grain materials bombarded by H, He and heavier atoms. Cuderman & Brady (1968), using ultra-high vacuum techniques ($5–10 \times 10^{-10}$ T), found the sputtering yield to be linearly proportional to the energy of the bombarding particle and concluded that the non-linearity of yield versus energy found by Stuart & Wehner (1962) at the lowest energies was due to the much higher residual gas pressure in that experiment ($10^{-6}–10^{-7}$ T), the effect of adsorbed gases being to decrease the yield.

The low-energy sputtering theories of Henschke (1957) and Aannestad (1973) predict a strong dependence of the yield upon the angle of incidence of the bombarding ion. However, the work of Cuderman & Brady (1968) shows that there is no dependence of the yield upon angle of incidence until the energy of the incoming particle exceeds about six times the threshold energy. Thus for $E < 6E_T = 24H_s$ we neglect any angular dependence of the sputtering yield. At higher energies, where an angular dependence begins to appear, the theory of Sigmund (1969) predicts that the yield should be proportional to $(\sec\theta)$ (where θ is the angle to the surface normal made by the incident particle) provided $m_i \ll M_s$, a condition which should be satisfied for most grain materials. With increasing θ the yield should eventually rapidly fall to zero as grazing incidence ($\theta = 90^\circ$) is approached. Almen & Bruce (1961) investigated the angular dependence of the sputtering yield for light ions up to $\theta = 60^\circ$ and found a $(\sec\theta)$ dependence for 45 KeV Ne^+ ions incident on Ag and Cu. The experimental work of Molchanov & Tel'kovskii (1961) for Ar^+ incident on Cu at 27 keV shows that the sputtering yield is proportional to $(\sec\theta)$ for $\theta \leqslant 70^\circ$, above which angle the yields falls rapidly. If Y is the yield for normally incident ions, we approximate the situation by requiring that for $E > 24H_s$:

$$\left.\begin{aligned} Y(\theta) &= Y(\sec\theta); \quad 0 \leqslant \theta \leqslant \pi/3 \\ Y(\theta) &= 2Y; \quad \pi/3 < \theta \leqslant \pi/2 \end{aligned}\right\}. \tag{4}$$

It can be shown that, for spherical grains and an isotropic or uniform flux of incident particles, an angular dependence given by (4) increases the average yield by a factor of 1.5. We note that Aannestad (1973) normalized his angular dependence theory to Wehner's (1959) experimental data on the sputtering of molybdenum by 800 eV Hg^+ ions; a case where the angular dependence is very much stronger than for low mass impinging ions (Sigmund 1969). Wehner (1959) finds virtually no angular dependence for the case of sputtering of Ag by 125 eV Hg^+ ions, supporting the conclusion of Cuderman & Brady (1968) that significant angular dependence does not set in until the incident energy exceeds at least six times the threshold energy.

Lagraeid & Wehner (1961) and Rosenberg & Wehner (1962) have determined the yield Y for a large variety of materials bombarded by ions of He^+, Ne^+, Ar^+ and Kr^+ having energies of 100, 200, 300 and 600 eV. We use this extensive collection of data to investigate if the quantities η_i or H_s influence the sputtering yield. We have determined, for a given incident ion and energy, (a) the range of values (the largest divided by the smallest), and (b) the ratio r (the mean divided by the standard deviation), for the following quantities: Y/E'; $Y/\eta_i E'$; $YH_s/\eta_i E'$ and YH_s/E', where $E' = (E - 4H_s)$. Table 2 displays the results for the representative cases of 300 eV ions of He^+, Ne^+ and Ar^+ incident on various materials. The yield data for He^+ ions was taken from Rosenberg & Wehner (1962) and that for Ne^+ and Ar^+ was taken from Lagraeid & Wehner (1961). From Table 2 and from the data available at other ion energies we conclude that, overall, the quantity YH_s/E' shows the smallest range in values and the largest value of r for the various ions. We thus arrive at our final expression for the sputtering yield of an ion i of energy E_i incident on a target with sublimation energy H_s

$$Y_i = \frac{S_i}{H_s}(E_i - 4H_s) \tag{5}$$

where we shall call the quantity S_i the sputtering yield factor. It would appear that, as with the threshold energy, the sputtering yield at low energies is independent of both the angle of incidence and η_i, and that both the yield and the threshold depend only on H_s, again suggesting a resonance process of energy transfer.

Table 2. Sputtering yield data.

Incident ion (300 eV)	He^+ (20 materials)				Ne^+ (28 materials)				Ar^+ (28 materials)			
Parameter	Y/E'	$Y/\eta_i E'$	$YH_s/\eta_i E'$	YH_s/E'	Y/E'	$Y/\eta_i E'$	$YH_s/\eta_i E'$	YH_s/E'	Y/E'	$Y/\eta_i E'$	$YH_s/\eta_i E'$	YH_s/E'
Range	50	50	44	25	7.3	9.6	9.6	4.8	7.6	9.5	7.6	6.6
Mean	1.9×10^{-4}	9.6×10^{-4}	4.0×10^{-3}	7.9×10^{-4}	1.7×10^{-3}	3.1×10^{-3}	1.6×10^{-2}	7.9×10^{-3}	2.7×10^{-3}	3.6×10^{-3}	1.9×10^{-2}	1.3×10^{-2}
Mean/standard deviation (r)	1.17	1.13	1.53	1.37	1.62	1.54	2.15	2.70	1.69	1.61	2.03	2.62

We have determined the sputtering yield factor S_i for ions of He^+, Ne^+ and Ar^+ incident on various targets at various energies, using the data of Lagraeid & Wehner (1961) and Rosenberg & Wehner (1962), and an average has been taken to obtain the mean value of S_i for each ion i. For He^+ we find, using 71 ion–target–energy combinations, that $S_{He} = 8 \times 10^{-4}$. For Ne^+ ions it is found that $S_{Ne} = 8 \times 10^{-3}$ and for Ar^+ ions $S_{Ar} = 1.3 \times 10^{-2}$. For graphite and iron the value S_{He} can be directly determined from the data, and it is found that $S_{He}(\text{graphite}) = 9 \times 10^{-4}$ and $S_{He}(\text{iron}) = 1.4 \times 10^{-3}$.

Besides helium, the principal bombarding particles of astrophysical interest are hydrogen and the CNO group. The results above show that $S_{Ne}/S_{He} = 10$. The ratio S_{CNO}/S_{He} should be slightly less, due to the trend for S_i to decrease with decreasing ion mass. Gronlund & Moore (1960) have determined the sputtering yield of silver under bombardment by 5 keV ions of He, N, O and Ne. They find that $Y(\text{Ne})/Y(\text{He}) = 11.5$, $Y(\text{O})/Y(\text{He}) = 9.3$ and $Y(\text{N})/Y(\text{He}) = 8.3$. We approximate the astrophysical situation by adopting $S_{CNO}/S_{He} = 10$, with an effective CNO abundance (by number) of 10^{-3} that of hydrogen.

Few sputtering experiments have been carried out using hydrogen as the bombarding particle. Of those that have, the most relevant is the work of Furr & Finfgeld (1970) who have determined the sputtering yield of gold bombarded by protons. At 500 eV, an energy which is in the hard-sphere regime for this ion–target combination (i.e. $E < E_A$), they found that $Y(H^+) = 2.95 \times 10^{-3}$. From Rosenberg & Wehner (1962), the yield of 500 eV He^+ ions incident on Au (again $E < E_A$) is 6×10^{-2}. Thus $S_{He}/S_H = 20$ for this ion–target combination. The only other data available for hydrogen sputtering are in the keV range. However, provided the comparison between H and He is carried out in the same energy regime (i.e. $E < E_A$ for both, or $E_A < E < E_B$ for both) the results should be of relevance here. Data for H^+ sputtering have been taken from KenKnight & Wehner (1964), utilizing the experimentally established fact that H_2^+ sputters like two protons with half the energy each and H_3^+ sputters like three protons with a third of the energy each (Gronlund & Moore 1960; KenKnight & Wehner 1964). The yields derived represent the flat maximum in the sputtering yield curve. The corresponding yield for He^+ was derived from the 600 eV He^+ sputtering data of Rosenberg & Wehner (1962), utilizing the knowledge that for He^+ ions the yield in the flat maximum is 1.5 times the yield at 600 eV (Wehner, KenKnight & Rosenberg 1963). For ten target materials it is found that the average value of $Y(He^+)/Y(H^+)$ is equal to 18. This backs up the hard-sphere regime data for 500 eV H^+ and He^+ ions incident on Au, and we thus adopt a general value of 20 for the ratio S_{He}/S_H. We note that Fig. 2 of Burke & Silk (1974) contains two data points representing the yield of graphite sputtered by H_2^+ and H_3^+ ions. These data points, taken from Wehner *et al.* (1963), are in fact the experimental yields for aluminium, experiments never having been carried out for hydrogen incident on graphite.* However, the conclusions reached by Burke & Silk remain essentially unchanged, although their adopted sputtering threshold energy for graphite is too high, i.e. 48.8 eV compared to (a) $E_T = 4H_s = 29.4$ eV, and (b) the experimentally determined threshold displacement energy of 31 eV for graphite surface atoms (Montet & Myers 1971), and 29.7 eV for interior graphite atoms (Montet 1973).

It has been suggested (e.g. Henschke 1957) that in the hard-sphere collision regime (i.e. low-energy sputtering) the magnitude of the sputtering yield will be proportional to the outer electron shell radii of the impinging particles, so that neutral atoms would have a higher yield than the corresponding ions, especially for hydrogen. However, the findings above throw serious doubts on all such dynamical arguments. An effect of the sort predicted by Henschke was thought to have been found by Weiss, Heldt & Moore (1958), but it was

* The high yields found by Feinberg & Post (1976) for *hot* graphite ($\geqslant$600 K) exposed to 600 eV H atoms are attributable to the chemical sputtering mechanism discussed in Section 1.2 of Paper II.

later found that the apparent increased yield that they found for H atoms compared to protons was in fact due to the presence of heavy neutral molecules in the H atom beam (Gronlund & Moore 1960). O'Briain, Lindner & Moore (1958) found that 9 keV protons incident on Ag had a sputtering yield approximately half that of H_2^+ ions of the same energy. Since H_2^+ ions dissociate on impact at that energy this implies that protons and H atoms have the same yield and that the electron shell radius is unimportant, a result supported by the H_2^+ and H_3^+ sputtering data of KenKnight & Wehner (1964) and the proton sputtering data of Furr & Finfgeld (1970). Thus in our calculations we adopt the same sputtering yield factor for atoms and ions of the same element.

In some astrophysical sputtering situations molecules of H_2 may be present. Although keV H_2 particles dissociate on impact and sputter as two H particles, this is unlikely to happen for the case of low-energy sputtering. In this situation H_2 molecules ought to show similar sputtering behaviour to deuterium atoms, which have the same mass. The data of Gronlund & Moore (1960) shows that the ratio of sputtering yields for D and H is 2.5. Thus, there is no need to allow explicitly for H_2 sputtering, since a hydrogen gas having a fraction $(1-f)$ of atomic H and a fraction $f/2$ of H_2 ($f \equiv 2n_{H_2}/n_H$) will sputter in essentially the same way as a gas entirely composed of atomic hydrogen.

All the conclusions above have been derived from sputtering yield data for monatomic solids, and it may be asked if the sputtering yield for compound materials will behave in the same manner. To answer this question an analysis has been carried out of the data of Comas & Cooper (1966) for Ar^+ ions incident on the semi-conductors PbTe, GaAs, InSb, CdS, GaP and SiC, and the data of Jorgenson & Wehner (1965) for Ar^+ ions incident on the insulator SiO_2. For the case of 300 eV Ar^+ ions, it is found that this group of materials shows exactly similar behaviour to that found above the monatomic solids investigated by Lagraeid & Wehner (1961). Jorgenson & Wehner (1965) found that solid SiO_2 was sputtered essentially as complete molecules, the average composition of the sputtered material being $SiO_{1.6}$. Wehner *et al.* (1963) found that the sputtering yields of a sample of terrestrial rocks were similar to that of iron, a material with a similar sublimation energy. We conclude that our sputtering treatment is valid for both monatomic and compound interstellar grains.

Table 3 displays the derived and adopted values of the sputtering yield factor S_i, for various gas particle species i and grain materials. Aannestad (1973) normalized his sputtering theory to Wehner's (1959) yield data for Hg^+ incident on Mo. As seen from Table 3 the sputtering yield factor S_i increases with increasing ion mass, and the equivalent value of S_i that would be derived from Wehner's (1959) data (after averaging over angle of incidence) is $S_i \approx 8 \times 10^{-2}$. This is a factor of 100 larger than that appropriate for helium sputtering and 2000 times larger than that appropriate for hydrogen sputtering.★

Table 3. Derived and adopted values for the sputtering yield factor S_i, for various grain materials and incident particles i.

Grain material	S_H	S_{He}	S_{CNO}
Graphite	4.5×10^{-5}	9×10^{-4}	9×10^{-3}
Iron	7×10^{-5}	1.4×10^{-3}	1.4×10^{-2}
All others	4×10^{-5}	8×10^{-4}	8×10^{-3}

★ After this work was completed, a paper by Taglauer *et al.* (1977) appeared containing low-energy sputtering data for H (and He and Ne) ions incident on Ni, at an angle 60° to the surface normal. For 100 eV ions, Fig. 4 of Taglauer *et al.* gives $Y(He) = 3.7 \times 10^{-2}$ and $Y(Ne) = 0.2$, compared to predicted yields of 3×10^{-2} and 0.3 from equations (4) and (5). For 250 eV ions $Y(H) = 1.8 \times 10^{-3}$, $Y(He) = 0.1$ and $Y(Ne) = 0.5$, compared to predicted yields of 4.2×10^{-3}, 8.4×10^{-2} and 0.84 respectively. Thus the predicted yields agree adequately with the experimental yields.

3.4 THERMAL SPUTTERING OF INTERSTELLAR GRAINS

Consider a spherical dust grain of radius a immersed in a gas with equipartition of energy and kinetic temperature T. If gas particle species i has a mass of m_i and number density n_i then the number of collisions per unit time made by gas species i with the grain is given by

$$n_i \left(\frac{m_i}{2\pi kT}\right)^{3/2} 4\pi a^2 \int_{\phi=0}^{2\pi}\int_{\theta=0}^{\pi/2}\int_{v=0}^{\infty} \exp\left(\frac{-m_i v^2}{2kT}\right) v^3\, dv \cos\theta \sin\theta\, d\theta\, d\phi$$

where θ is the angle to the surface normal. Each impinging particle will sputter Y_i lattice particles, provided $E_i = \frac{1}{2}m_i v^2 > 4H_s$, with Y_i given by equation (5). Therefore the number of particles sputtered from the grain surface per unit time by gas species i is given by

$$N_{sp}(i) = 4\pi a^2 n_i \left(\frac{m_i}{2\pi kT}\right)^{3/2} \frac{S_i}{H_s} \int_{\phi=0}^{2\pi}\int_{\theta=0}^{\pi/2}\int_{v=v(\mathrm{thr})}^{\infty} [\tfrac{1}{2}m_i v^2 - 4H_s]$$

$$\times \exp\left(\frac{-m_i v^2}{2kT}\right) v^3\, dv \cos\theta \sin\theta\, d\theta\, d\phi \qquad (6)$$

where the threshold velocity for sputtering by gas species i is given by

$$v(\mathrm{thr}) = \left(\frac{8H_s}{m_i}\right)^{1/2}. \qquad (7)$$

If each lattice particle has a mass M_s then the rate of loss of mass by the grain due to sputtering by gas species i is obtained by multiplying (6) by M_s. This mass-loss rate $|dm_g/dt|_i$ is also given by

$$\left|\frac{dm_g}{dt}\right|_i = 4\pi a^2 \rho_g \left|\frac{da}{dt}\right|_i \qquad (8)$$

where m_g is the mass of the grain and ρ_g is the mass density of the grain. Thus by multiplying (6) by M_s, integrating, and equating to (8) we obtain

$$\left|\frac{da}{dt}\right|_i = \frac{n_i M_s}{\rho_g}\left(\frac{kT}{2\pi m_i}\right)^{1/2} \frac{kT}{H_s} S_i \left[\frac{4H_s}{kT} + 2\right] \exp\left(\frac{-4H_s}{kT}\right). \qquad (9)$$

The rate of decrease of the grain radius due to sputtering by all gas particle species is given by

$$\left|\frac{da}{dt}\right| = \sum_i \left|\frac{da}{dt}\right|_i. \qquad (10)$$

In astrophysical situations the only important sputtering species are H, He and the CNO group. We adopt a helium abundance by number of 10^{-1} that of hydrogen and as discussed in the previous section take an effective CNO abundance by number of 10^{-3} that of hydrogen. Inspecting (9) we see that the only dependence of $|da/dt|_i$ on the species i is through the quantity $n_i S_i / m_i^{1/2}$. With the adopted abundances and the values of S_i given in Table 3 we see that H and He give identical contributions to the total sputtering rate. The CNO group on the other hand gives a contribution which is only 2.5 per cent that of the combined H and He contributions and so we neglect the CNO contribution for the case of *thermal* sputtering of grains. The total rate of decrease of radius of a grain due to sputtering

by all gas species in a gas of temperature T is thus given by

$$\left|\frac{da}{dt}\right| = \frac{2nM_s}{\rho_g}\left(\frac{kT}{2\pi m_H}\right)^{1/2}\frac{kT}{H_s}S_H\left[\frac{4H_s}{kT}+2\right]\exp\left(\frac{-4H_s}{kT}\right) \tag{11}$$

where n is the H nucleus number density, m_H is the mass of a H atom and S_H is the sputtering yield factor for H atoms incident on the particular grain material which has sublimation energy H_s and mass density ρ_g. Note that (11) applies only when the grain is uncharged or the gas is neutral. The effect of grain charging on sputtering in an ionized gas is dealt with in the next section.

Figs 1 and 2 display the quantity $1/n|da/dt|$ versus gas temperature T, for a number of different grain materials. When $3kT/2$ exceeds $24H_s$ we have taken into account a sputtering yield angular dependence given by (4) which for an isotropic flux of particles is equivalent to multiplying the value of $|da/dt|$ given by (11) by a factor of 1.5. For impinging particle energies above ~ 1 keV ($T \sim 10^7$K) the sputtering yield lies on a flat maximum. Sputtering by keV particles is dealt with in Section 4.

Table 4 displays the adopted values of H_s, M_s and ρ_g for the various grain materials. Note that for 'ice' grains the actual chemical composition and structure is irrelevant as far as sputtering is concerned, the sputtering yield depending only on the sublimation energy H_s. For silicates the parameters of enstatite ($MgSiO_3$) were taken as representative. The material

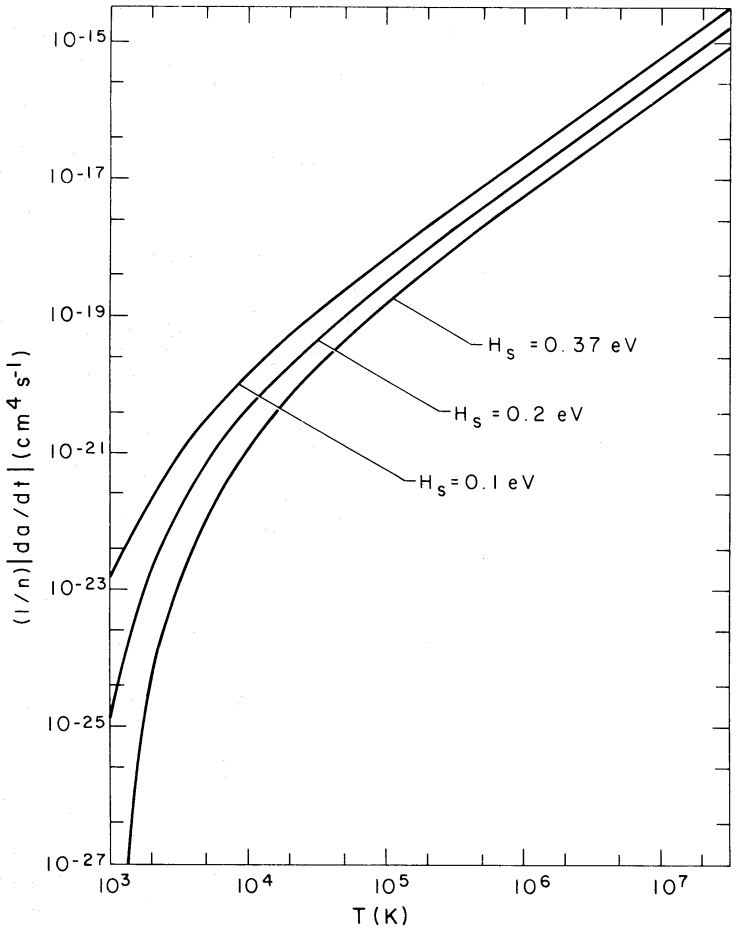

Figure 1. $(1/n)|(da/dt)|$, the rate of decrease of grain radius due to sputtering, divided by gas density, versus gas temperature T, for ice grains with three possible sublimation energies, H_s = 0.1, 0.2 and 0.37 eV.

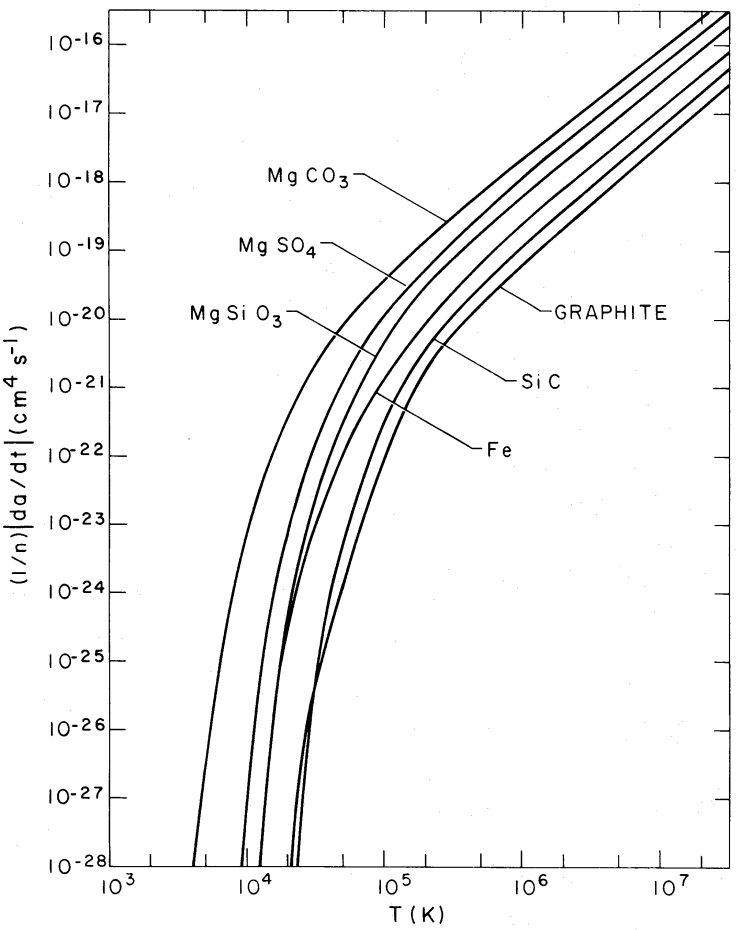

Figure 2. Sputtering rates $(1/n)|(da/dt)|$ versus gas temperature T, for six grain materials whose parameters are given in Table 4.

$MgCO_3$ has been proposed as an identification for a feature in the infrared spectra of several objects (Gillett, Forrest & Merrill 1973; Bregman & Rank 1975) and the material calcium magnesium sulphate has been proposed as explaining an emission feature at 8.7 μm in HD44179 (K. M. Merrill in Cohen *et al.* 1975). For the latter mentioned we assume that $MgSO_4$ is dominant on cosmic abundance grounds. Unfortunately, sublimation energy data were not available for $MgCO_3$ and $MgSO_4$, since both materials decompose on heating, with the evolution of CO_2 and SO_2 respectively. However, if we assume that the decomposition temperature gives a crude measure of the sublimation energy, we arrive at $H_s = 1.5$ eV for $MgCO_3$ and $H_s = 3.5$ eV for $MgSO_4$.

Table 4. Grain parameters of relevance to sputtering.

Grain material	H_s (eV)	ρ_g (g cm^{-3})	M_s/m_H
'Ice'	0.1	1.0	18
'Ice'	0.2	1.0	18
'Ice'	0.37	1.0	18
Graphite	7.35	2.2	12
Iron	4.3	7.9	56
Silicate ($MgSiO_3$)	4.5	3.2	100
Silicon carbide	7.8	3.2	40
$MgCO_3$	(1.5)	2.96	84
$MgSO_4$	(3.5)	2.66	120

The value of $1/n|da/dt|$ found here for ice grains with $H_s = 0.2$ eV in a gas with $T = 10^4$ K is 2.5 times larger than found by Barlow (1971). The main reason for the difference is that no angular dependence is assumed here for the threshold energy, leading to an effectively lower threshold energy.

3.5 SPUTTERING IN H II REGIONS, IN THE INTER-CLOUD MEDIUM AND BY SHOCK WAVES

Mathews (1969) has shown that in a H II region, where grains are charged due to photo-ejection and charged particle capture, lifetimes against sputtering for the uncharged case must be multiplied by a factor e^{γ}, where $\gamma = eV/kT$ is determined by the electrostatic potential of the grain V (i.e. positively charged grains have larger lifetimes). In a H II region with $T = 10^4$ K only ice grains will undergo significant physical sputtering. The lifetime of a charged ice grain with $H_s = 0.1$ eV and radius $a = 10^{-5}$ cm will be $3 \times 10^7 e^{\gamma}/n$ yr in a 10^4 K H II region with hydrogen number density n. Table 5 presents the lifetime of such a grain at various fractional Stromgren radii r/r_s, with grain charge parameters taken from Moorwood & Feuerbacher (1975), taking their results for Al_2O_3 as typical of dielectric grains. Lifetimes for grains with $H_s = 0.2$ eV and $H_s = 0.37$ eV can be found by multiplying those in Table 5 by 2.5 and 8, respectively.

The results of Mathews (1969) indicate that the dynamical lifetime of a H II region with $n = 10^4$ cm^{-3} should be of the order of 10^4 yr. Thus from Table 5 only ice grains at the outer edge of such a H II region would suffer significant destruction due to sputtering. The results for an $n = 10^2$ cm^{-3} H II region again indicate that only ice grains in the outer regions could suffer significant destruction due to sputtering during a typical dynamical lifetime of a few $\times 10^5$ yr. For the case of $n = 1$ cm^{-3} the lifetime of ice grains will be comparable to the main-sequence lifetime of the exciting stars. It would thus appear that only ice grains immersed in the outermost parts of dense H II regions can suffer significant destruction due to sputtering and then only over long timescales, a conclusion similar to that arrived at by Osterbrock (1974). We shall see in Section 3 of Paper II that there is a much more significant destruction mechanism than sputtering operative for ice grains in H II regions.

Greenberg & Hong (1974) have suggested that grains which acquire mantles in spiral arm clouds may be stripped of these mantles during passage through the hot inter-cloud medium, the passage taking about 10^8 yr. The exact temperature of the inter-cloud medium is uncertain at present with most estimates lying in the range 3000–8000 K. We shall adopt an inter-cloud temperature of 5000 K. Taking $n = 0.16$ cm^{-3} from Falgarone & Lequeux (1973), lifetimes for an uncharged ice grain of radius 10^{-5} cm equal to 6.4×10^8, 2.5×10^9 and 1.5×10^{10} yr are found for $H_s = 0.1$, 0.2 and 0.37 eV, respectively. Thus sputtering in an inter-cloud medium of this sort would appear to be unimportant.

Table 5. Sputtering lifetimes (in years) of ice grains of radius $a = 10^{-5}$ cm and sublimation energy $H_s = 0.1$ eV at various fractional Stromgren radii, r/r_s, in H II regions.

Spectral type of exciting star	Electron density (cm^{-3})	$r/r_s = 0.1$	$r/r_s = 0.5$	$r/r_s = 1.0$
O5	1	3.0×10^8	6.8×10^6	3.6×10^6
	10^2	2.5×10^7	1.6×10^5	6.4×10^4
	10^4	1.2×10^6	1.5×10^4	2.9×10^3
B0	1	1.7×10^8	5.6×10^6	3.6×10^6
	10^2	1.7×10^7	1.8×10^5	6.4×10^4

Jenkins & Meloy (1974) and York (1974) have suggested that O VI absorption lines seen in *Copernicus* spectra indicate the presence of a very hot rarified inter-cloud phase. Adopting mean parameters of $n = 8 \times 10^{-4}\,\mathrm{cm}^{-3}$ and $T = 5 \times 10^{5}\,\mathrm{K}$ from York (1974) the lifetimes of an ice grain of radius $10^{-5}\,\mathrm{cm}$ are found to be 5×10^{7}, 1×10^{8} and $1.9 \times 10^{8}\,\mathrm{yr}$ for $H_s = 0.1$, 0.2 and 0.37 eV, respectively. Since according to York's (1974) estimate only about 1 per cent by mass of the inter-cloud medium could be in this hot phase, we conclude that sputtering in such regions would be of no overall importance.

Another possible situation in which grains might be sputtered is in shock waves, caused for instance by cloud–cloud collisions or by expanding supernova remnants. After passing through a shock front a dust grain will have a macroscopic velocity v_M relative to the shocked gas, where v_M is the velocity of the shock front relative to the unshocked gas. The gas particles hitting the grain will therefore have a skewed Maxwellian velocity distribution in a frame co-moving with the grain (see also Aannestad 1973). Barlow (1975) has considered in detail the resultant sputtering rate. Only the results of that work are presented here.

Fig. 3 presents the total sputtering rate $1/n\,|da/dt|$ versus shock velocity v_M for ice grains with $H_s = 0.1$, 0.2 and 0.37 eV. The figure also presents, for $H_s = 0.37$ eV, the individual

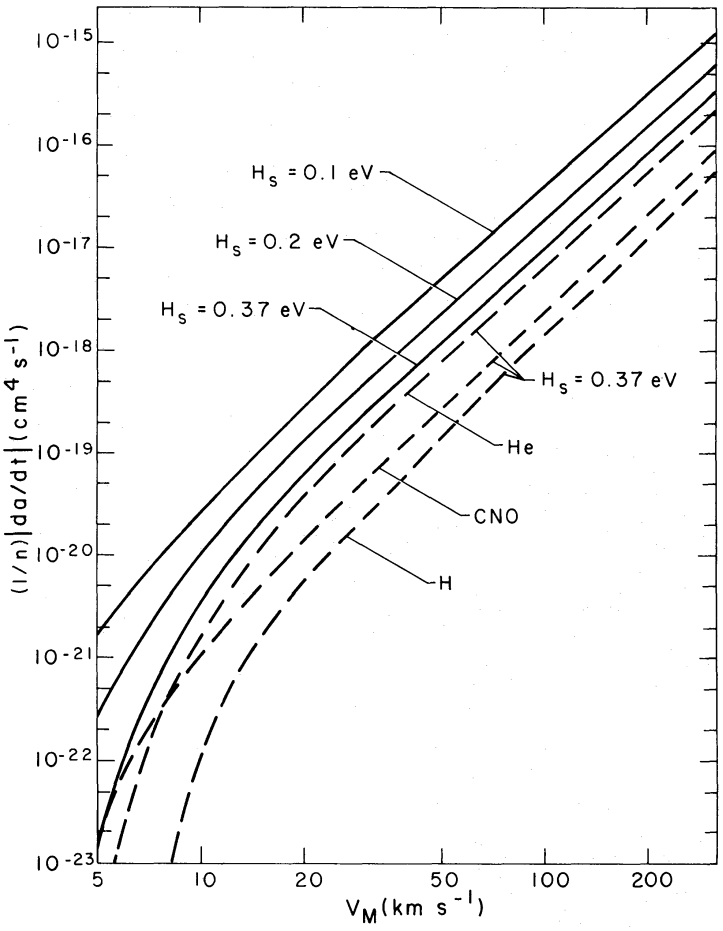

Figure 3. Sputtering rates $(1/n)|(da/dt)|$ versus V_M, for a grain moving with a velocity V_M relative to an adiabatically shocked gas whose temperature is given by (21). The solid lines show the total sputtering rates for ice grains with sublimation energies $H_s = 0.1$, 0.2 and 0.37 eV, respectively. The dashed lines illustrate the contributions to the sputtering rate of grains with $H_s = 0.37$ eV made by H, He and CNO atoms, respectively.

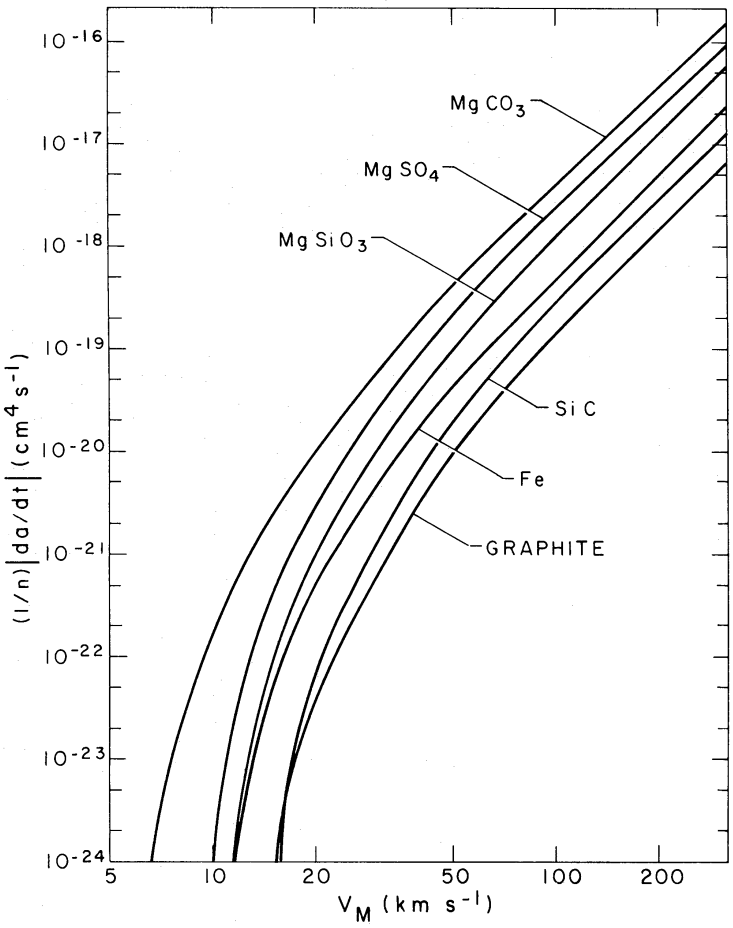

Figure 4. Total sputtering rates $(1/n)|(da/dt)|$ versus V_M, for six grain materials whose parameters are given in Table 4.

sputtering rates $1/n|da/dt|_i$ for i = H, He and CNO, for the relative abundances specified in Section 3.4. Fig. 4 gives only the total sputtering rate $1/n|da/dt|$ for the other grain materials specified in Table 4. For $(\frac{1}{2})m_i v_M^2 > 24H_s$ the yields in Figs 3 and 4 take account of a multiplying factor of 1.5 due to the angular dependence given by equation (4). The effects of grain charge on sputtering can of course be neglected for a neutral gas, although the gas will be ionized at the highest shock velocities. Inspection of Fig. 3 shows that, unlike the situation for a hot gas in equipartition, the CNO group makes a significant contribution to the total sputtering rate in a shock, whereas H atoms make only a maximum contribution of about 16 per cent to the total sputtering rate. The reason for this difference in behaviour is due to the fact that the sputtering rate for a particular incident particle is proportional to the product of its velocity v and energy $(\frac{1}{2})m_i v^2$. For a gas in equipartition the energy $(\frac{1}{2})m_i v^2$ is the same for all particles, so that v, and thus the sputtering rate, will be smaller for the more massive particles. On the other hand, for the case of a grain moving with a macroscopic velocity with respect to shocked gas, all particles have essentially the same velocity v with respect to the grain, so that $(\frac{1}{2})m_i v^2$, and thus the sputtering rate, will be larger for the more massive particles.

3.6 GRAIN LIFETIMES AGAINST SPUTTERING BY SHOCKS

The timescale for the slowing-down of a grain in a shock by gas kinetic drag, given by equation (14) below, is found always significantly to exceed the cooling timescale of the

shocked gas (Field *et al.* 1968; Aannestad 1973), for shock velocities $\lesssim 100$ km/s. Thus in estimating the fractional mass removed from a grain in a shock of velocity v we need only compare the destruction timescale with the grain slowing-down timescale.

For a grain of radius a (in cm) and sublimation energy H_s (in eV), travelling with velocity v (in km/s) relative to a gas with H nucleus number density n, the timescale for destruction by sputtering, $\tau_{dest}(v)$ can be shown, using (5), to be given approximately by

$$\tau_{dest}(v) = \frac{6 \times 10^{24} a H_s \rho_g}{n v^3 M_s} \text{ s}, \tag{12}$$

provided $v \geqslant v_{min} \simeq 16 H_s^{1/2}$ km/s (H_s in eV). M_s is the mass of a lattice particle (in units of m_H). The relative decrease in grain radius over a time t, as the grain velocity falls from an initial velocity v to a velocity v_{min} at time t_{min}, is given by

$$\frac{\Delta a}{a} = \int_0^{t_{min}} \frac{dt}{\tau_{dest}(v)}. \tag{13}$$

For a normal gas resistance law of the form

$$\frac{4}{3}\pi a^3 \rho_g \frac{dv}{dt} = -\pi a^2 \rho v^2, \tag{14}$$

where $\rho = \mu m_H n$ is the mass density of the shell material, we find, for $\mu = 1.4$, that

$$\frac{\Delta a}{a} = \int_{v_{min}}^{v} \frac{1.0 \times 10^{-6} M_s}{H_s} v\, dv = \frac{5.0 \times 10^{-7} M_s}{H_s} [v^2 - v_{min}^2], \tag{15}$$

with v and v_{min} in km/s and H_s, in eV. Thus for $v_{min} \sim 5$ km/s it is found that an initial shock velocity of $v = 100$ km/s is sufficient to destroy an ice grain with $H_s = 0.1$ eV. $H_s = 0.2$ eV requires $v = 140$ km/s. Setting $c = 5 \times 10^{-7} M_s/H_s$, we can express the fractional change in mass of a grain in a shock of velocity v, $\delta(v) = \Delta m_g/m_g$, as

$$\delta(v) = 1 - \left(1 - \frac{\Delta a}{a}\right)^3 = 3c(v^2 - v_{min}^2) - 3c^2(v^2 - v_{min}^2)^2 + c^3(v^2 - v_{min}^2)^3. \tag{16}$$

Thus an ice grain with $H_s = 0.1$ eV would lose half its mass ($\Delta a/a = 1/5$) in a shock with $v = 45$ km/s.

Consider now the sputtering of ice grains during cloud–cloud collisions. With the standard cloud parameters of Spitzer (1968), the rms relative velocity of two clouds is 20 km/s. A collision causes a shock to propagate back into each cloud and a grain entering the shocked region will have an rms initial velocity of 10 km/s with respect to the isothermally shocked gas. From equation (16), an ice grain with $H_s = 0.1$ eV will have a fraction $\delta = 1/50$ of its mass removed in each cloud collision and a grain with $H_s = 0.2$ eV will have a fraction $\delta = 1/150$ removed. For a mean time between cloud collisions of $\tau_{cc} = 6.5 \times 10^6$ yr (Spitzer 1968) we thus obtain lifetimes of 3.3×10^8 and 1×10^9 yr for ice grains with $H_s = 0.1$ and 0.2 eV, respectively (independent of grain radius).

Expanding supernova shells can also be effective in destroying interstellar grains. As discussed by Barlow & Silk (1977), the gas cooling timescale behind a shock increases significantly with increasing velocity, for shock velocities in excess of ~150 km/s, thus allowing complete destruction of refractory grains to take place in the hot shocked gas, even when their macroscopic velocity relative to the gas has fallen to low values. Following Barlow & Silk (1977) we define v_{sp} as the initial shock velocity above which complete

destruction of a grain will occur. For the purpose of estimating grain lifetimes against sputtering by supernova remnants we shall derive lifetimes against (1) complete destruction of a grain by a single remnant ($v \geqslant v_{sp}$) and (2) cumulative destruction by successive remnants ($v < v_{sp}$). The mean time for the destruction of a grain by a supernova remnant for case (1) is given by the mean time between supernova events in the Galaxy, τ_{SN}, multiplied by the effective volume of the Galaxy for supernova generation, divided by the volume of a remnant of radius R_{sp} when $v = v_{sp}$. For case (2) the lifetime is given by τ_{SN} multiplied by the effective volume of the Galaxy for supernova generation, divided by the volume of a remnant contained between radii R_{sp} and R_{min} (where $R = R_{min}$ when $v = v_{min}$) and divided also by $\bar{\delta}'$, the mean fractional mass of a grain removed in that volume.

Initial supernova remnant parameters are poorly known at present but we shall adopt a mean value of E_0/n (the initial energy of a supernova remnant divided by the local interstellar hydrogen number density) equal to 3×10^{50} erg cm^3, along with a mean time between supernova events in the Galaxy of $\tau_{SN} = 150$ yr. The lifetimes of grains for other values of these parameters can be obtained approximately by multiplying the lifetimes derived for the above values by $f = [3 \times 10^{50}\,\mathrm{erg\,cm^3}/(E_0/n)](\tau_{SN}/150\,\mathrm{yr})$. An effective galactic volume for supernova generation is assumed corresponding to a disc of radius 15 kpc and thickness 120 pc.

Table 6 presents the derived lifetimes against supernova sputtering. Column 1 lists the various grain materials. Column 2 gives the value of v_{sp} for each material. For ice grains the value of v_{sp} is independent of grain radius but for refractory grains v_{sp} is determined by the gas cooling curve and is *weakly* dependent on grain radius, as can be seen from Fig. 1 of Barlow & Silk (1977). For the purpose of the calculations in Table 6, representative grain radii of 3×10^{-6} cm were assumed for each of the four refractory grain materials. Column 3 of Table 6 presents R_{sp}, obtained from Shklovskii (1962) for the adiabatic expansion phase of a remnant and from equation (26) of Chevalier (1974) for the isothermal phase. Column 4 lists $\tau(1)$, the lifetime of a grain against complete destruction by a single remnant. Columns 5 and 6 present v_{min} and the corresponding radius R_{min}. For ice grains, v_{min} was set equal to 20 km/s, since below that point the remnant velocities merge with the random velocities of cloud motions, and destruction by sputtering during cloud collisions has already been taken into account earlier in this section. Column 7 gives $\bar{\delta}'$, the mean fractional mass of a grain removed inside the volume of a remnant contained between R_{sp} and R_{min}. The value of $\bar{\delta}'$ for each grain material was obtained using equation (A3) of Appendix A. Column 8 gives $\tau(2)$, the lifetime of a grain against cumulative destruction by successive remnants, Finally, column 9 lists τ(total), the lifetime of a grain against both (1) and (2).

The sputtering lifetimes of ice grains are independent of grain radius and from Table 6 it can be seen that these lifetimes are only weakly dependent on the sublimation energy. The lifetime of silicate grains is also independent of grain radius, because the value of v_{sp}

Table 6. Grain lifetimes against sputtering by supernova remnants.

Grain material	v_{sp} (km/s)	R_{sp} (pc)	$\tau(1)$ (yr)	v_{min} (km/s)	R_{min} (pc)	$\bar{\delta}'$	$\tau(2)$ (yr)	τ(total) (yr)
Ice (H_S = 0.1 eV)	100	18.5	4.8×10^8 f	(20)	38.1	0.30	2.1×10^8 f	1.5×10^8 f
Ice (H_S = 0.2 eV)	140	15.9	7.6×10^8 f	(20)	38.1	0.23	2.6×10^8 f	1.9×10^8 f
Ice (H_S = 0.37 eV)	190	13.9	1.1×10^9 f	(20)	38.1	0.18	3.2×10^8 f	2.5×10^8 f
$MgSiO_3$	230	12.2	1.7×10^9 f	34	30.0	0.17	7.1×10^8 f	5.0×10^8 f
Fe	250	11.6	2.0×10^9 f	33	30.4	0.12	9.5×10^8 f	6.4×10^8 f
SiC	270	11.0	2.3×10^9 f	45	26.5	0.073	2.5×10^9 f	1.2×10^9 f
Graphite	300	10.3	2.8×10^9 f	43	27.0	0.026	6.2×10^9 f	1.9×10^9 f

obtained from equation (15) is very close to the value of v_{sp} from Fig. 1 of Barlow & Silk (1977). For the rest of the refractory grains the sputtering lifetime is only weakly dependent on grain radius.

The value of $\tau_{SN} = 150\,\text{yr}$ used above was that derived by Clark & Caswell (1976) from radio SNR statistics. However, Tammann (1977) has arrived at a figure of $\tau_{SN} = 15\,\text{yr}$ for the Galaxy by taking the observed number of five supernovae in the last $10^3\,\text{yr}$ and multiplying by various proposed correction factors. Tammann's proposed supernova frequency would lead to a lifetime of only $5 \times 10^7\,\text{yr}$ for interstellar silicate grains. It is difficult to see how silicate grains could be replenished rapidly enough to match this destruction rate, since the timescale for recycling matter back to the interstellar medium via stars is believed to be significantly larger than a few times $10^7\,\text{yr}$.

4 The destruction of grains by keV and MeV particles

4.1 INTRODUCTION

In the keV to GeV energy regimes theoretical predictions are more in tune with the experimental data on sputtering and can thus be used to obtain estimates of likely destruction rates. The best understood sputtering mechanism in these energy regimes is the collision-cascade mechanism, whereby an impinging particle dislodges a lattice particle, giving it sufficient energy to displace other lattice particles, etc; a certain number of displaced particles eventually reach the surface and escape. De Jong & Kamijo (1973) for instance have presented estimates of sputtering rates for 0.1–10 MeV protons incident on ice grains, using the collision-cascade sputtering theory of Pease (1960). Collision-cascade sputtering is discussed in the next section.

A mechanism less well understood than collision-cascade sputtering is the thermal spike process, whereby energy is suddenly deposited in a localized and small volume of material, raising the temperature of the lattice significantly, so that evaporation of particles from the solid can take place if the heated spike volume intersects the surface. Thermal spikes might be caused by (a) knock-on lattice particles imparting a significant fraction of their kinetic energy to the lattice, or (b) the transferral of energy to the lattice by electrons produced in the ionization wake of a fast particle. Processes (a) and (b) have been considered by de Jong & Kamijo (1973) for the purpose of estimating the effects of cosmic rays on ice grains and Watson & Salpeter (1972) have considered the possible effect of process (b) in heating localized areas on the surfaces of refractory grains so as to cause the desorption of adsorbed particles. Sputtering via thermal spikes will be considered in Sections 4.3 and 4.4. Finally, the applications to the sputtering of grains by cosmic rays will be discussed in Section 4.5.

4.2 COLLISION-CASCADE SPUTTERING

The two most successful theories of collision-cascade sputtering are those of Pease (1960) and Sigmund (1969). The latter is the more rigorous theory and successfully predicts the energy and angular distribution of sputtered particles, something not attempted in the former theory. However, each theory gives equally good estimates for the sputtering yield (usually within a factor of 2–3 of experimental data), and since Sigmund's (1969) theory involves complex numerical terms, the more straightforward theory of Pease (1960) has been used to calculate sputtering yields.

The theory of Pease is successful in the weak-screening region ($E_A < E < E_B$) and in the Rutherford collision regime ($E > E_B$); where E_A and E_B are defined by

$$E_A = 2E_R Z_1 Z_2 (Z_1^{2/3} + Z_2^{2/3})^{1/2} (M_1 + M_2)/M_2 \tag{17a}$$

$$E_B = 4E_R^2 Z_1^2 Z_2^2 (Z_1^{2/3} + Z_2^{2/3})\, M_1/M_2 E_d. \tag{17b}$$

E_R is the Rydberg energy (13.6 eV), Z_1 and Z_2 are the atomic numbers and M_1 and M_2 the masses of the incident and target atoms respectively and E_d is the displacement energy of a lattice particle, taken here to be equal to $4H_s$ (see Section 3.2), where H_s is the sublimation energy of a lattice particle. This theory (and that of Sigmund 1969) is not successful in the hard-sphere collision regime ($E < E_A$) and so we do not apply is there.

For the sputtering yield Y Pease (1960) derives

$$Y = \sigma N_0^{2/3} \frac{\bar{E}}{4E_d} \left\{1 + \left[\frac{\ln(\bar{E}/H_s)}{\ln 2}\right]^{1/2}\right\} \tag{18}$$

where N_0 is the number density of lattice particles. In the weak-screening region ($E_A < E < E_B$)

$$\sigma = \pi a_0^2/(Z_1^{2/3} + Z_2^{2/3}) \tag{19}$$

and

$$\bar{E} = E_d \frac{E_B}{E} \ln\left(1 + \frac{4E^2}{E_A^2}\right) \tag{20}$$

where a_0 is the Bohr radius (5.29×10^{-9} cm).

In the Rutherford collision regime ($E > E_B$)

$$\sigma = 4\pi a_0^2 \frac{M_1}{M_2 E_d E} Z_1^2 Z_2^2 E_R^2 \left(1 - \frac{E_d}{E_{max}}\right) \tag{21}$$

and

$$\bar{E} = \frac{E_d}{(1 - E_d/E_{max})} \ln\left(\frac{E_{max}}{E_d}\right) \tag{22}$$

where

$$E_{max} = 4M_1M_2E/(M_1 + M_2)^2. \tag{23}$$

Table 7 presents the values of E_d, N_0, E_A and E_B for H, He and O incident on grains of graphite, iron and ice. The ice was assumed to be H_2O, with a discplacement energy of 0.4 eV, corresponding to the lowest likely sublimation energy of 0.1 eV. This is close to the estimate made by Fletcher (1970, p. 162) for the energy required to form a vacancy in H_2O ice. De Jong & Kamijo (1973) took an estimate of $E_d \sim 10$ eV for ice grains on the grounds that dissociation into atoms must take place before displacement can occur. However, the internal binding energy of a molecule does not contribute to the binding to other molecules in a solid. We assume here that for collisions of an incident particle with the *O nucleus* of a H_2O molecule the O atom behaves as a particle of atomic number 8 and atomic weight 18,

Table 7. Values of E_A and E_B for H, He and O incident on ice, graphite and iron.

Material	Ice			Graphite			Iron		
E_d (eV)	0.4			29.4			17.2		
N_0 (cm^{-3})	3.5×10^{22}			1.1×10^{23}			8.5×10^{22}		
Incident ion	H	He	O	H	He	O	H	He	O
E_A (keV)	0.514	1.26	9.30	0.37	0.96	8.2	2.25	4.88	26.0
E_B (keV)	32.9	5.88	539	0.32	5.85	559	5.08	86.1	6790

taking the H atoms with it (dissociation of the molecule might be caused by the electron excitation wake of the incident particle, the dominant mode of energy loss). For collisions of an incident particle with an *H nucleus* the H_2O molecule may indeed by dissociated, but then the efficiency of energy transfer between the knock-on H atoms and lattice H_2O molecules is very low. Since the theory of Pease (1960) assumes identical knock-on and lattice particle masses we therefore ignore the small contribution from knock-on H atoms. From de Jong & Kamijo (1973) we have adopted $N_0 = 3.5 \times 10^{22}\,\mathrm{cm}^{-3}$ for ice grains.

The case of silicate material is rather more complex than that of ice since here the atoms comprising the lattice molecules have comparable masses. We thus do not attempt to calculate a sputtering yield. Instead, we are guided by the experimental data of Wehner *et al.* (1963), which shows that (a) SiO_2 has a sputtering yield, for incident 7.5 keV H_2^+ and H_3^+ ions, identical to the yield found by KenKnight & Wehner (1964) for the same ions incident on iron, and (b) a wide variety of rock materials have yields similar to iron. Therefore we adopt the yields derived for iron as appropriate for silicates also.

Table 8 presents the yields calculated for H, He and O nuclei with $E > E_A$ incident on graphite, iron and ice. The yields presented are for back sputtering at the point of entry only. Transmission sputtering would occur at the exit point for particles with ranges significantly greater than the grain radius, doubling the theoretical yield. In addition, the sputtering theory of Sigmund (1969) predicts a $(\sec\theta)$ angular dependence for the yield in the keV region for light incident particles, and a $(\sec\theta)$ dependence in the MeV region for all incident particle masses. As discussed in Section 3.4 the available experimental data in the keV region confirms this. An angular dependence of the form given by equation (4) would produce a further increase in the mean yield by a factor of 1.5.

There is only a limited amount of experimental data available for comparison with the calculated sputtering yields presented in Table 8. The data of KenKnight & Wehner (1964), for H_2^+ and H_3^+ ions incident on iron, give a mean yield per 4 keV H nucleus of $Y = 10^{-2}$. The yield calculated from the Pease (1960) theory at this energy is $Y = 4 \times 10^{-2}$ (the yield calculated using the Sigmund (1969) theory is $Y = 5.8 \times 10^{-2}$). The data of Rosenberg & Wehner (1961), for 600 eV He^+ ions incident on graphite and iron, can be combined with the experimental datum that the maximum sputtering yield for helium is approximately 1.5 times the yield at 600 eV (Wehner *et al.* 1963). This gives a maximum experimental yield of 0.26 for He^+ incident on Fe, compared with a maximum yield from Table 8 of 0.42, and gives a maximum experimental yield of 0.13 for He^+ incident on graphite, compared with the maximum yield from Table 8 of 0.4. Almen & Bruce (1961) found a sputtering yield of 1.3 for 45 keV Ne^+ ions incident on Fe, compared with a predicted yield from equation (18) of $Y \sim 5$. The theoretical yields are therefore approximately a factor of 3 larger than the available experimental yields. Since in astrophysical situations the experimental yields for normal incidence would be increased by a factor of approximately 3 by transmission sputtering and angular dependence effects, the theoretical yields in Table 8 for back sputtering at normal incidence can be used as *total* mean yields for spherical grains.

The yields presented for ice in Table 8 are for a sublimation energy of 0.1 eV. The yield for any other ice sublimation energy H_s can be obtained approximately by multiplying the yields in Table 8 by $0.1/H_s$, with H_s in eV.

4.3 EVAPORATIVE SPUTTERING PRODUCED BY KNOCK-ON THERMAL SPIKES

A knock-on lattice particle, displaced by a primary impinging ion, expends about half of its energy in producing further displacements (Kinchin & Pease 1955) and the remainder of its energy is degraded into lattice thermal energy, appearing as a thermal spike (Seitz & Koehler

Table 8. Sputtering yields produced by collision-cascade sputtering.

	Ice (H_s = 0.1 eV)			Graphite			Iron (and silicates)		
E (eV)	Y_H	Y_{He}	Y_O	Y_H	Y_{He}	Y_O	Y_H	Y_{He}	Y_O
10^3	1.6	13.5		2.4×10^{-2}	0.40				
2×10^3	1.2	13		1.6×10^{-2}	0.34		4.7×10^{-2}		
5×10^3	0.63	8.5		8.8×10^{-3}	0.22		3.9×10^{-2}	0.42	
10^4	0.37	5.5	130	5.3×10^{-3}	0.10	3.0	2.4×10^{-2}	0.36	
2×10^4	0.23	3.4	110	3.2×10^{-3}	6.0×10^{-2}	2.4	1.5×10^{-2}	0.26	
5×10^4	0.10	1.6	70	1.5×10^{-3}	2.7×10^{-2}	1.5	7.3×10^{-3}	0.14	5.3
10^5	5.5×10^{-2}	0.90	44	8.3×10^{-4}	1.5×10^{-2}	0.91	4.2×10^{-3}	8.4×10^{-2}	3.9
2×10^5	2.9×10^{-2}	0.49	26	4.6×10^{-4}	8.2×10^{-3}	0.53	2.4×10^{-3}	4.6×10^{-2}	2.5
5×10^5	1.3×10^{-2}	0.22	12.7	2.1×10^{-4}	3.6×10^{-3}	0.25	1.1×10^{-3}	2.0×10^{-2}	1.3
10^6	6.9×10^{-3}	0.12	7.1	1.1×10^{-4}	1.9×10^{-3}	0.13	6.0×10^{-4}	1.1×10^{-2}	0.75
2×10^6	3.4×10^{-3}	5.3×10^{-2}	3.9	6.2×10^{-5}	1.0×10^{-3}	7.2×10^{-2}	3.2×10^{-4}	6.1×10^{-3}	0.42
5×10^6	1.5×10^{-3}	2.6×10^{-2}	1.7	2.7×10^{-5}	4.4×10^{-4}	3.1×10^{-2}	1.4×10^{-4}	2.6×10^{-3}	0.19
10^7	7.7×10^{-4}	1.3×10^{-2}	0.89	1.5×10^{-5}	2.5×10^{-4}	1.6×10^{-2}	7.8×10^{-5}	1.4×10^{-3}	9.9×10^{-2}
2×10^7	4.1×10^{-4}	7.0×10^{-3}	0.46	7.8×10^{-6}	1.3×10^{-4}	8.6×10^{-3}	4.2×10^{-5}	7.6×10^{-4}	5.2×10^{-2}
5×10^7	1.8×10^{-4}	3.0×10^{-3}	0.20	3.4×10^{-6}	5.7×10^{-5}	3.7×10^{-3}	1.8×10^{-5}	3.2×10^{-4}	2.2×10^{-2}
10^8	9.1×10^{-5}	1.6×10^{-3}	0.11	1.8×10^{-6}	3.0×10^{-5}	2.0×10^{-3}	9.6×10^{-6}	1.7×10^{-4}	1.2×10^{-2}
2×10^8	4.7×10^{-5}	8.1×10^{-4}	5.3×10^{-2}	9.4×10^{-7}	1.6×10^{-5}	1.0×10^{-3}	5.1×10^{-6}	9.1×10^{-5}	6.2×10^{-3}
5×10^8	2.0×10^{-5}	3.4×10^{-4}	2.3×10^{-1}	4.0×10^{-7}	6.8×10^{-6}	4.4×10^{-4}	2.2×10^{-6}	3.8×10^{-5}	2.6×10^{-3}
10^9	1.1×10^{-4}	1.8×10^{-4}	1.2×10^{-2}	2.1×10^{-7}	3.5×10^{-6}	2.3×10^{-4}	1.2×10^{-6}	2.0×10^{-5}	1.4×10^{-3}

1956). Evaporative sputtering by knock-on thermal spikes has been observed experimentally by Erents & McCracken (1973) for the case of keV H^+ and D^+ ions incident on a layer of solid H_2 deposited on a copper substrate (the results of Erents & McCracken are discussed in more detail in Section 4.4). A theory for evaporative sputtering from thermal spikes has been produced by Thompson & Nelson (1962). Following their treatment, we take the initial spike radius to be given by the range of the knock-on particle and use a mean spike lifetime determined by the diffusion coefficient of the solid material. The treatment given here differs from that of de Jong & Kamijo (1973), who assumed *point* deposition of heat at the initial location of the knock-on, thereby obtaining much higher temperatures initially than obtained here. The treatment of de Jong & Kamijo (1973) has the advantage of integrating numerically the sputtering yield during the time evolution of spike radius and spike temperature; the present treatment has the advantage of assuming initial deposition of heat over a finite volume.

The mean initial energy $\bar{E}$ of a knock-on lattice particle is given by (Pease 1960):

$$\bar{E} = E_d \frac{E_B}{E} \ln\left(1 + \frac{4E^2}{E_A^2}\right) \tag{24}$$

for the screened Coulomb regime ($E_A < E < E_B$) and

$$\bar{E} = \frac{E_d}{(1 - E_d/E_{max})} \ln\left(\frac{E_{max}}{E_d}\right) \tag{25}$$

for the Rutherford collision regime ($E > E_B$); where the various terms are as defined in Section 4.2.

The energy of the knock-on particle is always in the hard-sphere collision regime ($\bar{E} < E_A$, where E_A has a value appropriate for a lattice particle, of mass M_2 and atomic number Z_2, interacting with identical lattice particles). The range r_s of the knock-on is given by

$$r_s = (1/N_0)\, \sigma_{HS} \tag{26}$$

where N_0 is the number density of lattice particles and $\sigma_{HS} = \pi R^2$ is the hard-sphere collision cross-section, with R the solution of (Pease 1960):

$$R \frac{M_2}{M_1 + M_2} E = 2Z_1 Z_2 E_R a_0 \exp\left\{-\frac{(Z_1^{2/3} + Z_2^{2/3})^{1/2} R}{a_0}\right\}. \tag{27}$$

For the particular case of a knock-on colliding with identical lattice particles we have $M_1 = M_2$ and $Z_1 = Z_2$, so that with $Z_2 = 8$ and $M_2 = 18$ we obtain

$$R \exp\{2\sqrt{2}R/a_0\} = 128 E_R a_0/\bar{E}. \tag{28}$$

With half the knock-on energy available as heat, the mean energy E_0 given to each lattice particle in a spike of radius r_s is

$$E_0 = \frac{\bar{E}}{2} \Big/ \frac{4}{3} \pi r_s^3 N_0. \tag{29}$$

The temperature T_1 of the spike was obtained by Thompson & Nelson (1962) from the relation

$$\tfrac{3}{2} k T_1 = E_0 + \tfrac{3}{2} k T_0 \tag{30}$$

where T_0 is the ambient temperature of the solid. However, such a relation, which assumes freely interacting gas particles, is valid only for a disordered high-temperature region such as that considered by Thompson & Nelson (1962; $T_1 > 1700$ K in their experiment). For the present case equation (30) typically gives $T_1 \sim 300$ K; not high enough to justify a gas kinetic approximation. Instead, the lattice temperature is taken to be determined by the specific heat, as in Seitz & Koehler (1956), Chadderton & Torrens (1969) and Erents & McCracken (1973). For T_1 greater than the Debye temperature θ_D (a condition satisfied here since $\theta_D \sim 120$ K for a typical dirty-ice grain material according to de Jong & Kamijo 1973) use of the specific heat is equivalent to the equation (*cf.* Kittel 1966, p. 178).

$$3kT_1 = E_0 + 3kT_0. \tag{31}$$

From Thompson & Nelson (1962) a spike of radius r_s cools in a characteristic time τ_s, where

$$\tau_s = \frac{C_V}{4\kappa} r_s^2. \tag{32}$$

C_V is the specific heat (per unit volume) of the lattice material and κ is the thermal conductivity of the lattice material.

It is shown by Thompson & Nelson (1962) that the flux F of particles evaporating from the surface of a material of sublimation energy H_s, with energy in the interval dE at E, is given by

$$F = \left(\frac{2}{\pi M_2}\right)^{1/2} \frac{2N_0}{(kT_1)^{3/2}} \exp\left\{-\frac{(H_s + E)}{kT_1}\right\} E\, dE. \tag{33}$$

The probability $\bar{P}$ of a thermal spike of radius r_s intersecting the surface of a grain of radius a is given by $\bar{P} = 4r_s/\lambda$, for $r_s \ll a$. λ is the mean distance between displacement collisions. For $E_A < E < E_B$ we obtain from Pease (1960):

$$\lambda = (Z_1^{2/3} + Z_2^{2/3})/\pi a^2 N_0 \tag{34}$$

while for $E > E_B$:

$$\lambda = M_2 E_d E / 4\pi a_0^2 N_0 M_1 Z_1^2 Z_2^2 E_R^2 (1 - E_d/E_{max}). \tag{35}$$

The mean surface area $\bar{A}$ intersected by a spike is $\bar{A} = \frac{2}{3}\pi r_s^2$. Therefore, multiplication of F by $\bar{P}$, $\bar{A}$ and the spike lifetime τ_s gives the differential sputtering yield for this mechanism:

$$\frac{dY}{dE} = \frac{2}{3}\pi r_s^2 \frac{4r_s}{\lambda} \frac{C_V r_s^2}{4\kappa} \left(\frac{2}{\pi M_2}\right)^{1/2} \frac{2N_0}{(kT_1)^{3/2}} \exp\left\{-\frac{(H_s + E)}{kT_1}\right\} E. \tag{36}$$

Integrating over E between $E = 0$ and $E = \infty$ we obtain

$$Y = 4\frac{\pi}{3} r_s^5 \frac{C_V N_0}{\kappa\lambda} \left(\frac{2kT_1}{\pi M_2}\right)^{1/2} \exp\left(-\frac{H_s}{kT_1}\right). \tag{37}$$

Equation (37) has been evaluated for incident primary particles of H, He and O, with energy in the range 10^4–10^9 eV, for the case of the lowest likely ice sublimation energy, $H_s = 0.1$ eV, corresponding to $E_d = 0.4$ eV. We have adopted $T_0 = 20$ K. Table 9 presents the calculated yields Y, as well as λ, $\bar{E}$, r_s and T_1, for each case. $\kappa = 2.4 \times 10^5$ erg/cm/K/s and $C_V = 2.1 \times 10^7$ erg cm^{-3}/K have been adopted from the CRC Handbook of Chemistry and Physics, both of these values being appropriate for H_2O ice at ~ 250 K. In fact, for ice C_V is smaller and κ is significantly larger at lower temperatures of ~ 50 K (Klinger & Neumaier 1969; Fletcher

Table 9. Evaporative sputtering yields Y produced by knock-on collisions of H, He and O, in ice with sublimation energy H_S = 0.1 eV.

Incident particle	E (eV)	λ (cm)	$\bar{E}$ (eV)	r_S (Å)	T_1 (K)	Y
H	10^4	1.62×10^{-6}	9.63	9.39	174	1.7×10^{-3}
	10^5	4.94×10^{-6}	4.33	7.37	163	9.9×10^{-5}
	10^6	4.94×10^{-5}	5.25	7.80	166	1.5×10^{-5}
	10^7	4.94×10^{-4}	6.17	8.12	172	2.4×10^{-6}
	10^8	4.94×10^{-3}	7.09	8.54	170	2.8×10^{-7}
	10^9	4.94×10^{-2}	8.01	8.81	175	4.1×10^{-8}
He	10^4	1.81×10^{-6}	130.3	25.9	119	8.9×10^{-3}
	10^5	1.81×10^{-6}	23.9	12.7	174	6.7×10^{-3}
	10^6	3.09×10^{-6}	5.69	7.96	169	3.1×10^{-4}
	10^7	3.09×10^{-5}	6.61	8.33	171	4.2×10^{-5}
	10^8	3.09×10^{-4}	7.53	8.67	172	5.3×10^{-6}
	10^9	3.09×10^{-3}	8.45	9.00	173	6.7×10^{-7}
O	10^4	2.6×10^{-6}	3720	267	23	6.4×10^{-16}
	10^5	2.6×10^{-6}	1320	107	34	1×10^{-10}
	10^6	2.6×10^{-6}	231.5	34.5	94	1.8×10^{-3}
	10^7	2.6×10^{-6}	33.1	14.4	166	6.2×10^{-3}
	10^8	4.82×10^{-6}	7.73	8.72	174	3.8×10^{-4}
	10^9	4.82×10^{-5}	8.65	9.04	174	4.6×10^{-5}

1970) so that the evaporative sputtering yields presented in Table 9 are likely to be overestimates.

Comparison of the yields in Table 9 with those in Table 8 shows that evaporative sputtering by knock-on thermal spikes in ice grains can be neglected in comparison to sputtering produced by collision cascades.

The large yields ($Y \sim 10^4$) found by Erents & McCracken (1973) for 5–20 keV H^+ and D^+ ions incident in a layer of solid H_2 are due to a very much lower sublimation energy (H_S = 0.01 eV) for solid H_2 (they derive a spike temperature of only 50 K). The exponential dependence of Y upon H_S in (33) assures negligible yields for larger values of H_S.

4.4 THE EFFECT ON GRAINS OF ELECTRON EXCITATION ENERGY LOSS BY FAST PARTICLES

The dominant mode of energy loss in grains for impinging nuclei with energies in excess of a few keV is through electron excitation, leading to a tube of ionized matter along the path of the particle. If the ejected δ electrons can transfer their energy (~ 70 eV per electron for H_2O) to the lattice efficiently, then significant heating can take place, with subsequent evaporative sputtering. As noted by Watson & Salpeter (1972) and de Jong & Kamijo (1973), a major uncertainty is whether δ electrons can in fact transfer their energy to the lattice.

The transfer of energy between electrons and the lattice of a solid material is considered in detail by Chadderton & Torrens (1969), where it is shown that significant heating of the lattice can occur only in insulators. However, the insulators considered by Chadderton & Torrens were of high atomic weight, where δ electron energy loss through inelastic excitation of atoms will be unimportant. This will not be the case for insulators consisting of low mass molecules, where ionization or excitation can take place efficiently even for low electron energies (Charlesby 1960, p. 29). In this respect the experimental work of Erents &

McCracken (1973) is of crucial importance. They bombarded solid H_2 layers, deposited on a Cu substance, with keV protons, deuterons and electrons. For H_2 coverages of less than about 10 monolayers the high yields for 5–20 keV protons and deuterons ($Y \sim 10^4$) could be explained by knock-on thermal spikes in the Cu substrate (each spike having ~400 eV total energy and radius ~250 Å), which raised localized areas of the Cu surface to temperatures of ~50 K, thereby evaporating the H_2 on top. For higher coverages of H_2 the yield fell, reaching an approximately constant value ($Y \sim 25$–100) for coverages exceeding 10^3 monolayers ($\sim 3 \times 10^{-5}$ cm). Similar behaviour was found for 2 keV electrons, although yields were less than for the ionic case. For the high coverage cases the impinging ions and electrons lost their energy in the solid H_2, being unable to reach the Cu substrate to produce a thermal spike. The volume over which knock-ons are produced in solid H_2 being much larger than in Cu (~1000 Å radius versus ~250 Å radius) no concentrated heat was produced in the solid H_2 by knock-on thermal spikes. The observed high coverage yields therefore had to be explained by another mechanism (collision-cascade sputtering was found to give much too low a yield). Electron excitation effects were investigated by Erents & McCracken, who calculated that even if only 10 per cent of the energy lost through ionization and excitation was transferred to the lattice the yield would have been $Y \sim 10^4$, whereas the observed high coverage yields were a factor of 100 less. They found, however, that the high coverage yields could be explained by electrostatic effects, calculating for example that a 5 keV proton in solid H_2 would produce ionization events 50 Å apart, with a resultant electrostatic potential between ionic charges of 0.28 eV (the electrons are assumed to diffuse away), sufficient to desorb 25 molecules and in qualitative agreement with their experimental results. Support for this model came from the work of Clampitt & Gowland (1969), who detected the release of molecules in the form of ion clusters from electron bombarded H_2 and also from the work of Tantsyrev & Nikolaev (1972), who found ion clusters to be released from ion bombarded ice. (A similar mechanism had been proposed by Fleischer, Price & Walker (1965) in order to account for damage produced in dielectric materials by heavy ions. The process was termed an 'ion spike explosion'.)

It would appear that the energy lost by fast particles through ionization, dissociation and excitation does not get transferred to the lattice, for the case of light materials. Instead the initial δ electrons with an energy of ~70 eV lose most of their energy through further ionization, dissociation and excitation. Even when their energy falls to a level at which they can no longer excite molecules ($E < 5$–10 eV), no significant rise in lattice temperature is likely to be produced by the δ electrons, since the range of an electron with $E \sim 10$ eV is ~50 Å in H_2O (Spinks & Woods 1964, p. 245). When their energy becomes low enough the secondary electrons eventually neutralize ions or form negative ions by attachment to atoms or molecules (Lea 1955; Spinks & Woods 1964, p. 70). Thus practically all the energy lost by fast particles in dirty ice grains should reappear as discrete photons. This would therefore tend to rule out the possibility of thermal spikes being produced in ice grains via transfer to the lattice of energy lost in electron excitation.

4.5 GRAIN DESTRUCTION BY COSMIC RAYS

The possible destruction of full-grown ice grains by cosmic rays has been considered by de Jong & Kamijo (1973), who found that such a mechanism would only be significant if there existed a large flux of low energy cosmic rays (~2 MeV per nucleon), which were able in some way to produce sputtering yields of $Y \sim 1$ per H nucleus (evaporative sputtering from thermal spikes produced by electron excitation was proposed). We have argued in Section 4.4 that the energy lost to electron excitation by fast particles will not in fact be transferred

to the lattice for low atomic weight materials such as ice, and that collision-cascade sputtering yields should be used instead.

Taking sputtering yields for ice grains ($H_s = 0.1$ eV) from Table 8, for 2 MeV protons, 8 MeV α particles and 32 MeV oxygen nuclei, we obtain, for abundance ratios H:He:O = 10^3:10^2:1, a yield of $Y = 6 \times 10^{-3}$ per incident proton. With $\tau = 4a\rho_g/FYM_s$, we obtain $\tau = 2 \times 10^{11}$ yr for $a = 10^{-5}$ cm, $\rho_g = 1$ g cm^{-3}, $F = 36$ cm^{-2}/s (equivalent to the flux adopted by de Jong & Kamijo 1973) and $M_s = 18\, m_H$. However, the flux of 2 MeV protons adopted above was that postulated by Field, Goldsmith & Habing (1969) in order to produce an H atom ionization rate in the interstellar medium of $\zeta_H = 4 \times 10^{-16}$/s. More recent observational constraints, reviewed by Spitzer & Jenkins (1975), indicate that $\zeta_H \leqslant 10^{-16}$–$10^{-17}$/s, consistent with ionization only by the known cosmic ray flux spectrum, which peaks at ~100 MeV/nucleon. Since the total integrated flux from such a spectrum is less than the 2 MeV proton flux used above and since the mean energy per cosmic ray is higher (leading to a lower mean sputtering yield), collision-cascade sputtering of interstellar ice grains by cosmic rays of mean energy around 100 MeV/neutron can obviously be neglected. Significant destruction of ice grains by electron excitation temperature spikes can be definitely ruled out for a cosmic-ray spectrum with mean energy of about 100 MeV/nucleon, even if *all* of the energy of the ejected electrons could be transferred to the lattice. This can be shown as follows. If the mean distance λ_e between primary ionization events in the grain is less than four times the penetration distance r_e of the ejected primary electrons (a value of $r_e \sim 20$ Å for 70 eV electrons is deduced from Fig. 3.4 of Charlesby (1960), this being the radius in which most of the energy is lost) then the spherical temperature spikes of radius r_e can be treated as a single cylindrical tube of radius r_e. The evaporative sputtering yield is then obtained by a simple modification of equation (37) to be

$$Y = \pi r_e^4 \frac{C_V N_0}{\kappa} \left(\frac{2kT_1}{\pi M_2}\right)^{1/2} \exp\left(-\frac{H_s}{kT_1}\right). \tag{38}$$

For $\lambda_e > 4r_e$ equation (37) applies, with r_s replaced by r_e. It is found that (38) applies for protons with $E < 5$ MeV, α particles with $E < 100$ MeV and O nuclei with $E < 10$ GeV. The temperature T_1 of the cylinder of heated lattice material would be given by $T_1 = (E_0/3k) + T_0$, with $E_0 = \frac{1}{2}(-dE/dx)/\pi r_e^2 N_0$, where the factor of ½ takes account of the fact that about half the cosmic-ray energy is lost in overcoming the ionization potentials during the primary ionizations. The evaporative sputtering yield obviously peaks where $(-dE/dx)$ peaks, and this corresponds to an energy of 0.2 MeV for protons in ice, 1 MeV for α particles in ice, and 10 MeV for O nuclei in ice. It is found that the evaporative sputtering yield thus calculated is greater than the collision-cascade sputtering yield only for protons with $E < 2$ MeV, α particles with $E < 50$ MeV, and O nuclei with $E < 5$ GeV. Thus only for the case of O nuclei could a cosmic-ray spectrum peaking at around 100 MeV/nucleon give an evaporative sputtering yield larger than the collision-cascade yield. 100 MeV per nucleon O nuclei (i.e. $E = 1.6$ GeV) have an energy loss rate in ice of 380 MeV/cm. This would give a maximum evaporative sputtering yield of $Y = 0.7$. For a flux of protons of mean energy 100 MeV equal to 10 cm^{-2}/s and an [O]/[H] cosmic-ray abundance ratio of 10^3 we obtain a lifetime against destruction by 1.6 GeV O nuclei of 6×10^{12} yr, for ice grains with radius $a = 10^{-5}$ cm.

Ejection of ion clusters from ice by ion spike explosions can probably be neglected for cosmic rays of mean energy around 100 MeV/nucleon, since the mean distance between primary ionization events is then $\gtrsim 200$ Å for H and He nuclei and $\geqslant 20$ Å for O nuclei.

In the unlikely event that (a) low energy cosmic rays exist with a mean energy of 2 MeV per nucleon and a flux of $F = 36$ cm^{-2}/s, and (b) all electron excitation energy loss could be

transferred to lattice particles, it is found that an ice grain with $H_s = 0.1$ eV and radius 10^{-5} cm would have a lifetime of 6×10^8 yr. This number is obtained as a result of a yield $Y = 10^{-3}$ for 2 MeV protons, $Y = 10$ for 8 MeV α particles and $Y = 10^3$ for 32 MeV O nuclei; equivalent to a yield of $Y = 2$ per incident proton.

It has been suggested by Spitzer (1968, p. 156) and by de Jong & Kamijo (1973) that low energy cosmic rays with $E \sim 2$ MeV/nucleon could prevent the condensation of small ice grain nuclei in interstellar space if the total energy lost in a grain by a cosmic ray was greater than the total sublimation energy of the grain. However, if the electronic energy loss could not be transferred to the lattice then this conclusion would not hold. If there is no significant flux of low energy cosmic rays then the observed cosmic-ray flux above ~100 MeV/nucleon would be unable to prevent growth of nuclei, even if the energy lost could be converted into thermal energy, since it can be shown that there is too low a frequency of primary ionization events (which deposit ~70 eV of electronic kinetic energy each) to act as a significant destruction mechanism.

X-rays will interact with grains primarily via the photoelectric effect, ejecting an energetic electron. Calculations show that even if the entire photoelectron energy were to be transferred to the lattice, no significant evaporation would occur. For example, 0.25 keV soft X-rays eject photoelectrons with energy ~235 eV from H atoms. From Charlesby (1960, Fig. 3.4) the penetration of electrons with that energy, in material with a density and composition very similar to that of dirty ice (tissue), is 50 Å, giving a temperature rise of only 48 K if all the energy could be transferred to the lattice; with a resultant negligible yield using equation (37). Higher energy photons have a lower flux, a lower photoelectric cross-section and eject a higher energy photoelectron, whose larger penetration assures a smaller increase in lattice temperature.

Acknowledgments

I would like to thank Dr J. Silk for discussions on several aspects of this work and Professor M. W. Thompson for discussions on thermal spike mechanisms. During the early phases of this research numerous interesting discussions were held with D. R. Brand, J. C. Papaloizou and G. J. Vaughan. I thank Professor R. J. Tayler for his encouragement during the course of this work, which formed part of an unpublished DPhil thesis submitted to the University of Sussex in 1975. The work was begun during the tenure of a Northern Ireland Ministry of Education Research Studentship and was essentially completed during the tenure of an SRC Research Fellowship. I thank each of these organizations for their financial support.

References

Aannestad, P. A., 1973. *Astrophys. J. Suppl.*, **25**, 223.
Almen, O. & Bruce, G., 1961. *Nucl. Instr. Methods*, **11**, 257.
Barlow, M. J., 1971. *Nature Phys. Sci.*, **232**, 152.
Barlow, M. J., 1975. Unpublished *DPhil thesis*, University of Sussex.
Barlow, M. J. & Silk, J., 1977. *Astrophys. J. Lett.*, **211**, L83.
Bregman, J. D. & Rank, D. M., 1975. *Astrophys. J. Lett.*, **195**, L125.
Burke, J. R. & Silk, J., 1974. *Astrophys. J.*, **190**, 1.
Chadderton, L. T. & Torrens, I. McC., 1969. *Fission damage in crystals*, Methuen and Company, London.
Charlesby, A., 1960. *Atomic radiation and polymers*, Pergamon Press, Oxford.
Chevalier, R. A., 1974. *Astrophys. J.*, **188**, 501.
Clampitt, R. & Gowland, L., 1969. *Nature*, **223**, 815.

Clark, D. H. & Caswell, J. L., 1976. *Mon. Not. R. astr. Soc.*, **174**, 267.
Cohen, M., Anderson, C. M., Cowley, A., Coyne, G. V., Fawley, W. M., Gull, T. R., Harlan, E. A., Herbig, G. H., Holden, F., Hudson, H. S., Jakoubek, R. O., Johnson, H. M., Merrill, K. M., Schiffer, F. H., Soifer, B. T. & Zuckerman, B., 1975. *Astrophys. J.*, **196**, 179.
Comas, J. & Cooper, C. B., 1966. *J. Appl. Phys.*, **37**, 2820.
Cuderman, J. F. & Brady, J. J., 1968. *Surface Sci.*, **10**, 410.
Danielson, R. E., Woolf, N. J. & Gaustad, J. E., 1965. *Astrophys. J.*, **141**, 116.
Erents, S. K. & McCracken, G. M., 1973. *J. Appl. Phys.*, **44**, 3139.
Falgarone, E. & Lequeux, J., 1973. *Astr. Astrophys.*, **25**, 253.
Feinberg, B. & Post, R. S., 1976. *J. Vac. Sci. Tech.*, **13**, 443.
Field, G. B., Goldsmith, D. W. & Habing, H. J., 1969. *Astrophys. J. Lett.*, **155**, L149.
Field, G. B., Rather, J. D. G., Aannestad, P. A. & Orszag, S. A., 1968. *Astrophys. J.*, **151**, 953.
Fleischer, R. L., Price, P. B. & Walker, R. M., 1965. *J. Appl. Phys.*, **36**, 3645.
Fletcher, N. H., 1970. *The chemical physics of ice,* Cambridge University Press.
Furr, A. K. & Finfgeld, C. R., 1970. *J. Appl. Phys.*, **41**, 1739.
Gillett, F. C. & Forrest, W. J., 1973. *Astrophys. J.*, **179**, 483.
Gillett, F. C., Forrest, W. J. & Merrill, K. M., 1973. *Astrophys. J.*, **183**, 87.
Gillett, F. C., Jones, T. W., Merrill, K. M. & Stein, W. A., 1975. *Astr. Astrophys.*, **45**, 77.
Greenberg, J. M. & Hong, S.-S., 1974. *Proc. IAU Symp. 60,* p. 13, eds Kerr, F. J. & Simonson, S. C., D. Reidel, Dordrecht, Holland.
Gronlund, F. & Moore, W. J., 1960. *J. Chem. Phys.*, **31**, 1132.
Harrison, D. E. & Magnusson, G. O., 1961. *Phys. Rev.*, **122**, 1421.
Henschke, E. B., 1957. *Phys. Rev.*, **106**, 737.
Hoyle, F. & Wickramasinghe, N. C., 1962. *Mon. Not. R. astr. Soc.*, **124**, 417.
van de Hulst, H. C., 1943. *Ned. Tijdschr. v. Natuur.*, **10**, 251.
Hunter, C. E. & Donn, B., 1971. *Astrophys. J.*, **167**, 71.
Jenkins, E. B. & Meloy, D. A., 1974. *Astrophys. J. Lett.*, **193**, L121.
de Jong, T. & Kamijo, F., 1973. *Astr. Astrophys.*, **25**, 363.
Jorgenson, G. V. & Wehner, G. K., 1965. *J. Appl. Phys.*, **36**, 2672.
Kamijo, F., 1963. *Publ. astr. Soc. Japan,* **15**, 440.
KenKnight, C. E. & Wehner, G. K., 1964. *J. Appl. Phys.*, **35**, 322.
Kinchin, G. H. & Pease, R. S., 1955. *Rep. Prog. Phys.*, **18**, 1.
Kittel, C., 1966. *Introduction to solid state physics,* J. Wiley and Sons, New York.
Klinger, J. & Neumaier, K., 1969. *C. R. Acad. Sci.*, **B269**, 945.
Knacke, R. F., Cudaback, D. & Gaustad, J. E., 1969. *Astrophys. J.*, **158**, 151.
Lagraeid, N. & Wehner, G. K., 1961. *J. Appl. Phys.*, **32**, 365.
Langberg, E., 1958. *Phys. Rev.*, **111**, 91.
Lea, D. E., 1955. *Actions of radiations on living cells,* Cambridge University Press.
Mathews, W. G., 1969. *Astrophys. J.*, **157**, 583.
Molchanov, V. & Tel'kovskii, V., 1961. *Sov. Phys. Doklady,* **6**, 137.
Montet, G. L., 1973. *Carbon,* **11**, 89.
Montet, G. L. & Myers, G. E., 1971. *Carbon,* **9**, 179.
Moorwood, A. F. M. & Feuerbacher, B., 1975. *Astrophys. Sp. Sci.*, **34**, 137.
O'Briain, C. D., Lindner, A. & Moore, W. J., 1958. *J. Chem. Phys.*, **29**, 3.
Oort, J. H. & van de Hulst, H. C., 1946. *B.A.N.*, **10**, 187.
Osterbrock, D. E., 1974. *Astrophysics of gaseous nebulae,* W. H. Freeman, San Francisco.
Pease, R. S., 1960. *Rend. SIF XIII,* p. 158.
Rosenberg, D. & Wehner, G. K., 1962. *J. Appl. Phys.*, **33**, 1842.
Seitz, F., 1949. *Disc. Faraday Soc.*, **5**, 271.
Seitz, F. & Koehler, J. S., 1956. *Solid State Phys.*, **2**, 305.
Shklovskii, I. S., 1962. *Astr. Z.*, **39**, 209 (*Sov. Astr.*, **6**, 162, 1962).
Sigmund, P., 1969. *Phys. Rev.*, **184**, 184.
Spinks, J. W. T. & Woods, R. J., 1964. *An introduction to radiation chemistry,* J. Wiley and Sons, New York.
Spitzer, L., 1968. *Diffuse matter in space,* Interscience.
Spitzer, L. & Jenkins, E. B., 1975. *A. Rev. Astr. Astrophys.*, **13**, 133.
Stuart, R. V. & Wehner, G. K., 1962. *J. Appl. Phys.*, **33**, 2345.
Taglauer, E., Marin, G., Heiland, W. & Beitat, U., 1977. *Surf. Sci.*, **63**, 507.
Tammann, G. A., 1977. In *Supernovae,* p. 95, ed. Schramm, D. N., D. Reidel, Dordrecht, Holland.

Tantsyrev, G. D. & Nikolaev, E. N., 1972. *Dokl, Akad. Nauk SSSR*, **206**, 151.
Thompson, M. W. & Nelson, R. S., 1962. *Phil. Mag.*, 7, 2015.
Watson, W. D. & Salpeter, E. E., 1972. *Astrophys. J.*, **174**, 321.
Wehner, G. K., 1957. *Phys. Rev.*, **108**, 35.
Wehner, G. K., 1958. *Phys. Rev.*, **112**, 1120.
Wehner, G. K., 1959. *J. Appl. Phys.*, **30**, 1762.
Wehner, G. K., KenKnight, C. & Rosenberg, D. L., 1963. *Plan. Sp. Sci.*, **11**, 885.
Weiss, A., Heldt, L. & Moore, W. J., 1958. *J. Chem. Phys.*, **29**, 7.
Wickramasinghe, N. C., 1965. *Mon. Not. R. Astr. Soc.*, **131**, 177.
Wickramasinghe, N. C., 1972. *Mon. Not. R. astr. Soc.*, **159**, 269.
York, D. G., 1974. *Astrophys. J. Lett.*, **193**, L127.

Appendix A: the mean fractional mass of a grain sputtered by a supernova remnant

Consider an expanding supernova remnant in which momentum is conserved. We have

$$M = k/v \tag{A1}$$

where M and v are the mass and expansion velocity of the remnant and k is a constant. $\delta(v)$, the fractional mass of a grain destroyed by a shock of initial velocity v, is given by equation (16) of Section 3.6. The volume-weighted mean value of $\delta(v)$ in the remnant, $\bar{\delta}'$, for the mass swept up between the times when $v = v_{sp}$ and $v = v_{min}$ is given by

$$\bar{\delta}' = \frac{\int_{M(v_{sp})}^{M(v_{min})} \delta(v)\, dM}{\int_{M(v_{sp})}^{M(v_{min})} dM} = \frac{\int_{v_{min}}^{v_{sp}} (1/v^2)\, \delta(v)\, dv}{[(1/v_{min}) - (1/v_{sp})]}. \tag{A2}$$

Substituting for $\delta(v)$ from (16) and integrating we obtain

$$\bar{\delta}' = \left\{3c(v_{sp} - v_{min}) - c^2(v_{sp}^3 - v_{min}^3) + \frac{c^3}{5}(v_{sp}^5 - v_{min}^5) + (6c^2v_{min}^2 + 3v_{min}^4c^3)(v_{sp} - v_{min}) \right.$$
$$\left. - c^3v_{min}^2(v_{sp}^3 - v_{min}^3)\right\} \Big/ \left(\frac{1}{v_{min}} - \frac{1}{v_{sp}}\right) - (3cv_{min}^2 + 3c^2v_{min}^4 + c^3v_{min}^6). \tag{A3}$$